3-Substituted Indazoles as Configurationally Locked 4EGI-1 Mimetics and Inhibitors of the eIF4E/eIF4G Interaction

8 AUTHORS, INCLUDING:

Revital Yefidoff-Freedman
Brigham and Women's Hospital
9 PUBLICATIONS **85** CITATIONS

SEE PROFILE

Rupam Sahoo
Harvard Medical School, Brigham and Wom…
25 PUBLICATIONS **239** CITATIONS

SEE PROFILE

Limo Chen
University of Texas MD Anderson Cancer Ce…
18 PUBLICATIONS **147** CITATIONS

SEE PROFILE

Michael Chorev
Harvard University
252 PUBLICATIONS **6,709** CITATIONS

SEE PROFILE

3-Substituted Indazoles as Configurationally Locked 4EGI-1 Mimetics and Inhibitors of the eIF4E/eIF4G Interaction

Revital Yefidoff-Freedman,[a, b] Ting Chen,[a, b] Rupam Sahoo,[a, b] Limo Chen,[a] Gerhard Wagner,[c] Jose A. Halperin,[a, b] Bertal H. Aktas,[a, b] and Michael Chorev*[a, b]

4EGI-1, the prototypic inhibitor of eIF4E/eIF4G interaction, was identified in a high-throughput screening of small-molecule libraries with the aid of a fluorescence polarization assay that measures inhibition of binding of an eIF4G-derived peptide to recombinant eIF4E. As such, the molecular probe 4EGI-1 has potential for the study of molecular mechanisms involved in human disorders characterized by loss of physiological restraints on translation initiation. A hit-to-lead optimization campaign was carried out to overcome the configurational instability in 4EGI-1, which stems from the *E*-to-*Z* isomerization of the hydrazone function. We identified compound **1a**, in which the labile hydrazone was incorporated into a rigid indazole scaffold, as a promising rigidified 4EGI-1 mimetic lead. In a structure–activity relationship study directed towards probing the structural latitude of this new chemotype as an inhibitor of eIF4E/eIF4G interaction and translation initiation we identified **1d**, an indazole-based 4EGI-1 mimetic, as a new and improved lead inhibitor of eIF4E/eIF4G interaction and a promising molecular probe candidate for elucidation of the role of cap-dependent translation initiation in a host of pathophysiological states.

Introduction

Protein–protein interactions (PPIs) are ubiquitous and serve critical roles in many biological systems. By nature, the interacting interfaces of the two macromolecules are large—(1940 ± 760) Å^{2} [1]—and shallow with scattered binding hotspots that provide most of the binding energy. In comparison with inhibition of enzyme–substrate or receptor–ligand interactions, disruption of PPIs by small molecules presents an ambitious challenge.[2] Nevertheless, targeting of PPIs by chemical biology approaches to develop effective small-molecule probes and potential drug candidates should advance our understanding of the involvement of PPIs in normal biology and pathobiology, and dramatically expand the druggable genome, allowing for new therapeutic approaches.[3] In recent years this approach has yielded some successful small-molecule PPI inhibitors that have been promoted into clinical trials.[4]

Translation, the process of protein biosynthesis, consists of three stages: initiation, elongation, and termination. Translation initiation (TI), a highly regulated process governed by numerous eukaryotic TI factors (eIFs), results in the assembly of elongation-competent 80S ribosome on the initiation codon.[5] The PPIs between eIF4E and eIF4G, which are the focus of our studies, are essential for cap-dependent translation, by which most mammalian mRNAs are translated. In cap-dependent translation, an mRNA cap (m^{7}GpppN, 7-methylguanosine-5′-triphosphonucleotide) structure is recognized by eIF4E, the cap-binding protein.[6] eIF4E interacts with eIF4G, a scaffolding protein; this also interacts with eIF4A, an RNA helicase, to form the eIF4F complex.[5, 7] Interaction of eIF4G with the dorsal side of eIF4E is centered on a conserved hydrophobic motif formed by the sequence $Y(X)_4L\Phi$, where X can be any amino acid and Φ is any hydrophobic amino acid. The eIF4E/eIF4G interaction (and, by extension, formation of the eIF4F complex) is regulated by eIF4E-binding proteins (4E-BPs), which contain the same hydrophobic motif as eIF4G and compete with eIF4G for binding to eIF4E. Hyperphosphorylation of 4E-BPs by the mammalian target of rapamycin complex 1 (mTORC1) reduces their affinity for eIF4E, thus allowing for binding of eIF4E to eIF4G and formation of the eIF4F complex. The eIF4F complex binds the mRNA and 40S ribosomal subunit in addition to other TI factors and unwinds the secondary structures in the 5′-untranslated (5′UTR) region of mRNA to scan for the initiator AUG codon where the 40S ribosomal subunit is joined by the 60S subunit, thus forming the translation-competent 80S ribosome on the start codon.

In most normal cells, the low abundance of eIF4E relative to other eIFs[8] and its interaction with 4E-BPs turns it into a rate-

[a] *Dr. R. Yefidoff-Freedman, Dr. T. Chen, Dr. R. Sahoo, Dr. L. Chen, Prof. Dr. J. A. Halperin, Prof. B. H. Aktas, Prof. M. Chorev Laboratory for Translational Research, Harvard Medical School 240 Longwood Avenue, Boston, MA 02115 (USA) E-mail: michael_chorev@hms.harvard.edu*

[b] *Dr. R. Yefidoff-Freedman, Dr. T. Chen, Dr. R. Sahoo, Prof. Dr. J. A. Halperin, Prof. B. H. Aktas, Prof. M. Chorev Hematology Laboratory for Translational Research Brigham and Women's Hospital, Harvard Medical School 20 Shattuck Street, Thorn 7, Boston, MA 02115 (USA)*

[c] *Prof. G. Wagner Department of Biological Chemistry and Molecular Pharmacology Harvard Medical School 240 Longwood Avenue, Boston, MA 02115 (USA)*

Supporting information for this article is available on the WWW under http://dx.doi.org/10.1002/cbic.201300723.

limiting factor for the cap-dependent translation.[9] However, this balance is functionally perturbed in many diseased states. Regulation of the eIF4F activity plays a critical role in normal biology, whereas its perturbation contributes to the pathobiology of many human disorders. The eIF4F complex is critically required for cellular proliferation, differentiation, and survival.[10] It also plays a critical role in long-term memory consolidation[11] and is implicated in the pathobiology of human disorders including autism,[12] fragile-X syndrome,[13] tuberous sclerosis,[14] and some cancers. Autism is thought to be caused by increased translation of synaptic mRNA.[15] Dysregulation of synaptic protein synthesis might result from genetic alterations in the components of the eIF4F complex, its negative regulators (4E-BPs), or activation of upstream signaling pathways that elevate eIF4F activity. The most prominent example of these pathways is signaling by the mammalian target of rapamycin (mTOR), which is itself regulated by the interplay of phosphoinositide 3-kinase (PI3K)/protein kinase B (Akt), phosphatase, and tensin homologue (PTEN). Various genetic aberrations that lead to activation of mTOR are associated with autism spectrum disorders.[16] Importantly, many symptoms of autism spectrum disorders can be reversed by inhibiting mTOR activity[17] or by pharmacologically inhibiting the formation of the eIF4F complex.[12b] Another mental disorder, fragile-X syndrome, is caused by defects in the functioning of the cytoplasmic fragile-X mental retardation protein (FMRP) interacting protein 1, which is an eIF4E-binding protein that suppresses eIF4F-driven cap-dependent translation.[18] Tuberous sclerosis complex (TSC) is involved in a group of disorders caused by mutations in the tuberin and hamartin genes that lead to uncontrolled activation of mTOR and thereby eIF4F complex formation and unrestricted translation.[19] TSC disorders include benign tumors of lung, kidney, brain, and other organs and autism spectrum disorders. At the molecular level TSC is associated with activation of eIF4F as well as uncontrolled endoplasmic reticulum stress. The involvement of eIF4F complex in numerous pathological states highlights the urgent need for better pharmacological probes for the study of the role of this complex in normal biology and pathobiology. Such probes might also provide a launching pad for the development of therapeutic agents for various inflammatory, proliferative, and neurodegenerative disorders.

We discovered 4EGI-1 (Scheme 1) in a high-throughput screening campaign employing a fluorescence polarization (FP) assay that searched chemical libraries for small molecules that would bind to eIF4E and compete with a fluorescence-labeled eIF4G-derived peptide.[20] 4EGI-1 binds to eIF4E, disrupts eIF4E/eIF4G interaction, and inhibits cap-dependent TI in vitro and growth of human cancer xenografts in vivo.[20] Preliminary SAR (structure–activity relationship) studies highlighted the critical role of the hydrazone function in the minimal pharmacophore of 4EGI-1.[20a] However, although the hydrazone is essential for 4EGI-1's inhibitory activity, it introduces inherent configurational instability, and this is a major liability in controlling chemophysical properties and achieving defined and preselected biological activities. E-to-Z isomerization around the C=N bond is affected by solvents, solutes, pH, and temperature, making the
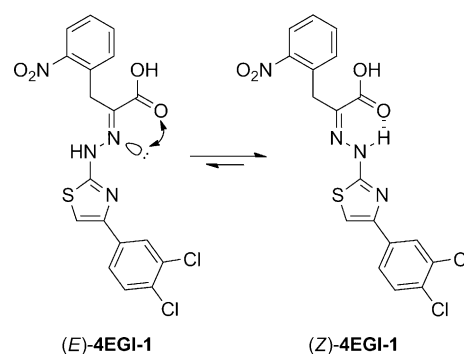
Scheme 1. E-to-Z isomerization of 4EGI-1.

more stable and slightly more hydrophobic Z isomer the predominant isomer. This isomerization phenomenon, observed in a wide range of hydrazones of different nature, is extensively documented in the literature.[21]

To overcome the configurational lability in 4EGI-1, we sought to eliminate the isomerization around its hydrazone function. Evidently, ring closure between the NH of the hydrazone (CH=N-**NH**-) and the ortho position of the benzyl moiety, which is recapitulated closely in an indazole system (Scheme 2)
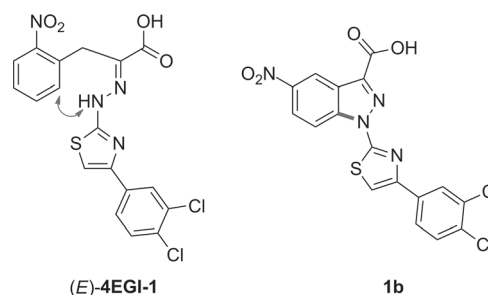
Scheme 2. Rigidifaction of the configuration of (E)-4EGI-1 around the C=N−N− bond in a 3-substituted indazole scaffold, a true (E)-4EGI-1 mimetic.

should be a suitable solution: in this chemotype, the hydrazone becomes an integral part of an indazole scaffold—a condensed bicyclic system—and is locked in the E configuration, so the potential isomerization around the C=N−N− bond is blocked. As such, 1-[4-(3,4-dichlorophenyl)thiazol-2-yl]-5-nitro-1H-indazole-3-carboxylic acid (**1b**) is structurally a rigidified (E)-4EGI-1 mimetic.

Natural products containing indazole cores are quite rare, nevertheless, indazole appears as a privileged scaffold in several bioactive compounds of diverse therapeutic significance,[22] such as antidepressants,[23] contraceptives,[24] anticoagulants,[25] anti-HIV agents,[26] agents for treatment of metabolic syndromes,[27] analgesics,[28] anticancer drugs,[29] and chronic obstructive pulmonary disease therapeutics.[30]

In a recent study, an indazole core was introduced to configurationally lock, and thus mimic, an X-ray-derived target-bound conformation of a parent small molecule that is a potent inhibitor of reverse transcriptase.[26] This rigidification resulted in increased potency, specificity, and excellent phar-

macokinetics. However, not all attempts to introduce an indazole ring into a bioactive compound result in improved activity. Incorporating the hydrazone function of a potent phosphodiesterase-4 inhibitor into the pyrazole ring of an indazole system resulted in significant loss of potency. This loss was attributed to the steric hindrance imposed by the indazole ring disrupting binding at the catalytic site.[30]

Herein, we report the synthesis of a new class of configurationally constrained 4EGI-1 mimetics in which the hydrazone function is locked in an E configuration as part of an indazole-based cyclic scaffold and their evaluation as inhibitors of eIF4E/eIF4G interaction and of cap-dependent TI.

Results and discussion

Chemistry

The two synthetic approaches we employed in the preparation of the indazole-based constrained mimetics of the (E)-4EGI-1 library are outlined in Scheme 3. The first was a convergent synthesis in which two fragments—a 1H-indazole-3-carboxylic acid and a 2-halo-4-phenylthiazole—were combined through a regioselective N-arylation to yield the final 4EGI-1 mimetic (Scheme 3, route a); the second was a linear synthesis in which a 4EGI-1-like hydrazone was assembled in a stepwise manner followed by intramolecular cyclization, involving the N-arylation of the NH of the hydrazone, to generate the anticipated indazole-containing 4EGI-1 mimetic (Scheme 3, route b).

In the convergent synthesis pathway (Scheme 3, route a), the preparation of the 2-halo-4-phenylthiazolyl fragments was carried out by a well-documented pathway. Firstly, the bromoacetophenones **2 a–h** were transformed into the corresponding thiocyanatoacetophenones by treatment with potassium thiocyanate[31] and subsequently underwent intramolecular cyclization upon treatment with either gaseous HCl or HBr,

to generate the corresponding 2-halo-4-phenylthiazoles[32] **4 a–h** in moderate yields (Scheme 4). Nitration of 1H-indazole-3-carboxylic acid in fuming nitric acid yielded the other fragment, 5-nitro-1H-indazole-3-carboxylic acid.[33] Subsequent N-arylation of the indazole (or 5-nitroindazole) in the presence of powdered sodium hydroxide in DMSO by 2-halo-4-phenylthiazole **4** at 110 °C afforded the anticipated indazole-derived 4EGI-1 mimetics (**1′ a–c** and **1 a–g**) in low to moderate yields (Scheme 4). Replacement of bromoacetophenones **2 a–g** with 2-bromo-1-phenylpropan-1-one (**2 h**) also led to the introduction of a methyl group on C-5 of the thiazolyl ring (Scheme 4).

The second strategy for the synthesis was developed with the goal of obtaining higher yields of the focused 3-substituted indazole library of compounds **1** (Scheme 3, route b). The synthetic pathway was designed to generate derivatives of 2-(2-bromo(-5-nitro)phenyl)-2-[(4-arylthiazol-2-yl)hydrazono]acetic acid (compounds **7**) that would form the fused pyrazole ring (i.e., indazole) through intramolecular cyclization (Scheme 5). The transformation of arylhydrazones, usually formed by condensation of a hydrazine derivative and either a 2-substituted benzaldehyde or ketone, into indazoles is well established. This intramolecular aromatic nucleophilic substitution, with emphasis on the appropriate reaction conditions (dictated by the leaving group and the hydrazine moiety), is extensively documented in the literature.[22, 25, 34]

In the first step of this pathway we utilized a Hantzsch-type reaction[35] between thiosemicarbazide[36] and α-halo-substituted acetophenones **2 a–d**, **2 g**, or **2 i**—**t** or 2-bromo-1-phenylpropan-1-ones **2 h** or **2 u**. In most cases this led to the formation of two cyclic products: the desired 2-hydrazinyl-4-phenylthiazoles **5 a–d**, **5 g**, or **5 i–t** or the 2-hydrazinyl-4-phenyl-5-methylthiazole **5 h** or **5 u**, together with the irrelevant 6-phenyl-6H-1,3,4-thiadiazin-2-amines **5***.[36] These side products **5* a–u** were formed in variable quantities, in several cases equal to those of the desired five-membered ring intermedi-
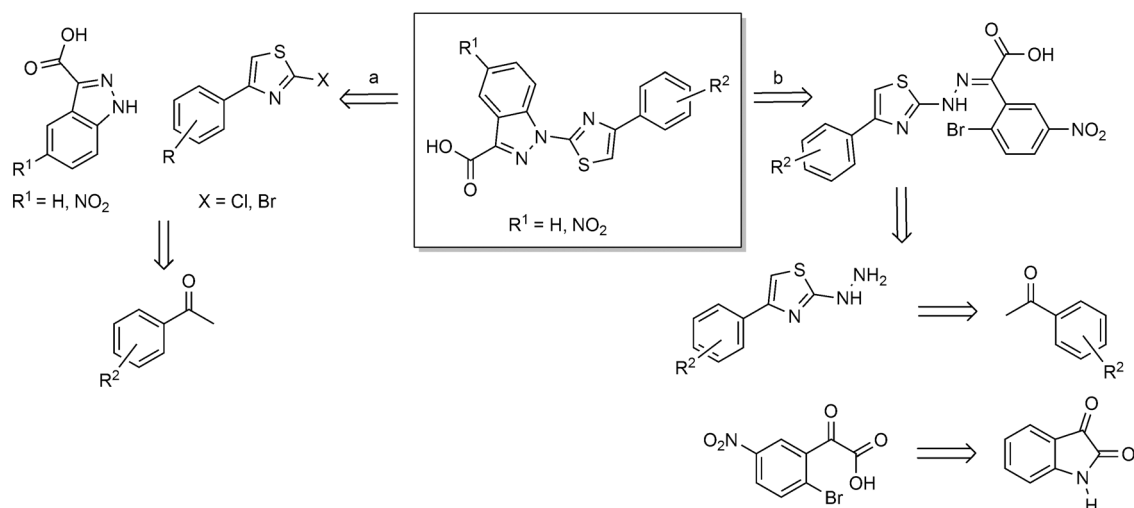
Scheme 3. Retrosynthetic analysis of the two strategies for the preparation of 3-substituted indazoles as configurationally constrained 4EGI-1 mimetics. a) Convergent synthesis combines two independently synthesized building blocks, the 1H-indazole-3-carboxylic acid and a 2-halo-4-phenylthiazole. b) Linear synthesis that assembles in a stepwise manner a linear precursor that in the final step undergoes an intramolecular reaction to generate the anticipated constrained indazole-based 4EGI-1 mimetic.
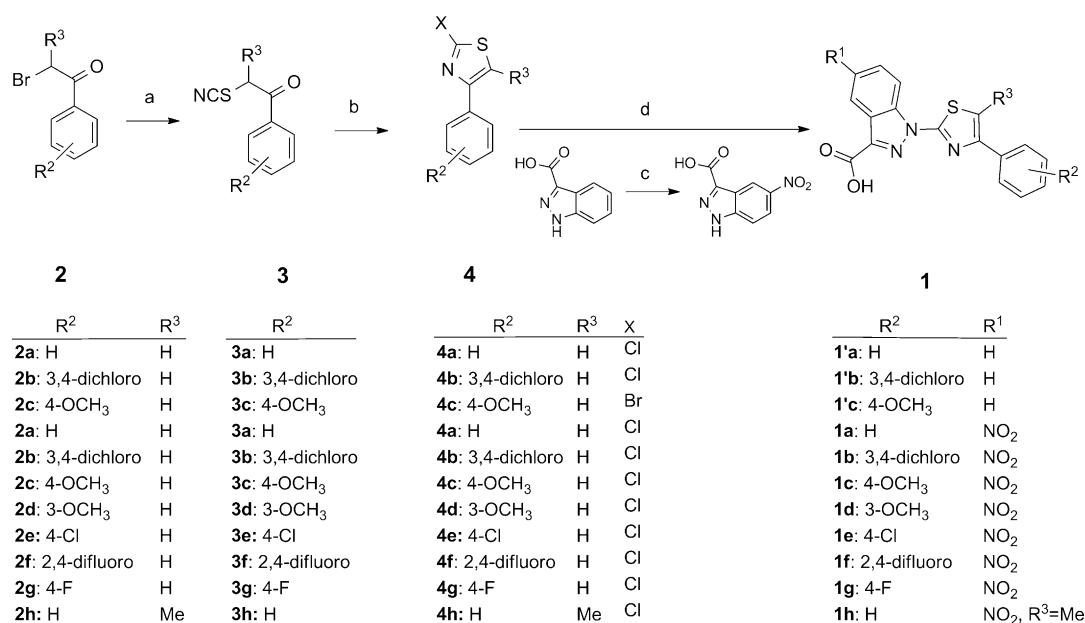
Scheme 4. Convergent synthesis of indazole-based constrained 4EGI-1 mimetics through N-arylation of 1H-indazole-3-carboxylic acids with 2-halo-4-phenyl-thiazoles. Reagents and conditions: a) KSCN (2 equiv), acetonitrile, reflux, overnight; b) gaseous HCl or HBr, dry ether, 0 °C to RT, overnight; c) HNO$_3$/H$_2$SO$_4$ (conc.); d) 1H-indazole-3-carboxylic acid or 5-nitro-1H-indazole-3-carboxylic acid, NaOH (2.2 equiv) in DMSO, N$_2$.

ates **5a–u**. For characterization purposes we isolated a few of the 2-aminothiadiazines **5*** (e.g., **5*a**, **5*k**, **5*m**; see the Experimental Section) and confirmed their structural integrity. Practically, we were able to use the crude mixtures containing both **5** and **5*** and to subject them to subsequent condensation with oxoacetic acid derivatives **6**, obtaining the same yield of hydrazones **7** as in preparations in which we used isolated hydrazines **5**. This synthetic shortcut is possible because the 2-aminothiadiazines **5*** are weaker nucleophiles than the 2-hydrazinyl-4-phenylthiazoles **5** and cannot compete in the condensation reactions. Moreover, the disparity in polarity between compounds **5*** and compounds **7** is much greater than that between compounds **5*** and compounds **5**, thus making the isolation of **7** by chromatography a straightforward task.

Of note is the lack of understanding of the anticipated product distribution in Hantzsch reactions between α-halocarbonyl-containing compounds and thiosemicarbazide. Many studies report the formation of mixtures of 2-hydrazinyl-4-phenylthiazole and 2-aminothiadiazine derivatives, similarly to what we have observed.[37] On the other hand, there are reports on reaction conditions that lead to the exclusive formation of 2-aminothiadiazine derivatives.[36,38] In the absence of systematic studies that provide mechanistic insight into the different reaction pathways we remain unable to control the reaction course to generate the five-membered-ring compounds as the exclusive or predominant products.

A three-step transformation of isatin into the critical 2-(2-bromo-5-nitrophenyl)-2-oxoacetic acid (**6**, Scheme 5) was accomplished by two previously reported procedures involving nitration of isatin[39] and subsequent basic hydrolysis to provide the related 2-(2-amino-5-nitrophenyl)-2-oxoacetic acid.[40] For the last step we adapted the Sandmeyer reaction to convert the aromatic amine into **6**. Condensation of the 2-hydrazinyl-4-

phenylthiazoles **5** with the 2-(2-bromo-5-nitrophenyl)-2-oxo-acetic acid (**6**) generated the targeted linear precursor 2-(2-bromo-5-nitrophenyl)-2-[(4-arylthiazol-2-yl)hydrazono]acetic acids **7**. In general, we obtained mixtures of (E)- and (Z)-hydrazones in which the E forms were predominant (>94%). The major isomer was isolated and purified for characterization in each case, but this was not essential: monitoring of the intramolecular cyclization reaction by HPLC-MS indicated that both isomers in the mixture were fully consumed and transformed into the anticipated indazole **1**. We assume that dynamic Z-to-E isomerization under the conditions of the cyclization explains the disappearance of the Z isomers. Our arylhydrazones **7** required a combination of base (Na$_2$CO$_3$/N,N′-dimethylethylene-diamine) and CuI used as a catalyst; this has proven successful in many N-arylation reactions.[41] This combination allowed the synthesis of the indazole-based constrained (E)-4EGI-1 mimetic library **1** (Scheme 5) with moderate to excellent yields.

Comparison of the two synthetic pathways shows that, in spite of the larger number of synthetic steps, the linear synthesis is better than the convergent one. In almost all cases we obtained better yields of the same 3-substituted indazoles (e.g., **1g**—47% vs. 12%; **1a**—30% vs. 21%; and **1b**—34% vs. 14%). The N-arylation step that combines the two fragments, the 5-nitroindazoles and compounds **4a–h** (route a in Scheme 3) is the main culprit for the lower overall yield of the convergent synthetic pathway. Taken together, our synthetic work generated a focused library of pure (>95% by RP-HPLC) indazole-based constrained (E)-4EGI-1 mimetics **1a–u**, established their structural integrity by ^{1}H and ^{13}C NMR and HRMS, and laid the synthetic groundwork for further structural optimization.

Introduction of a nitro group at C-5 of the indazole ring compromised the solubilities of these compounds: whereas
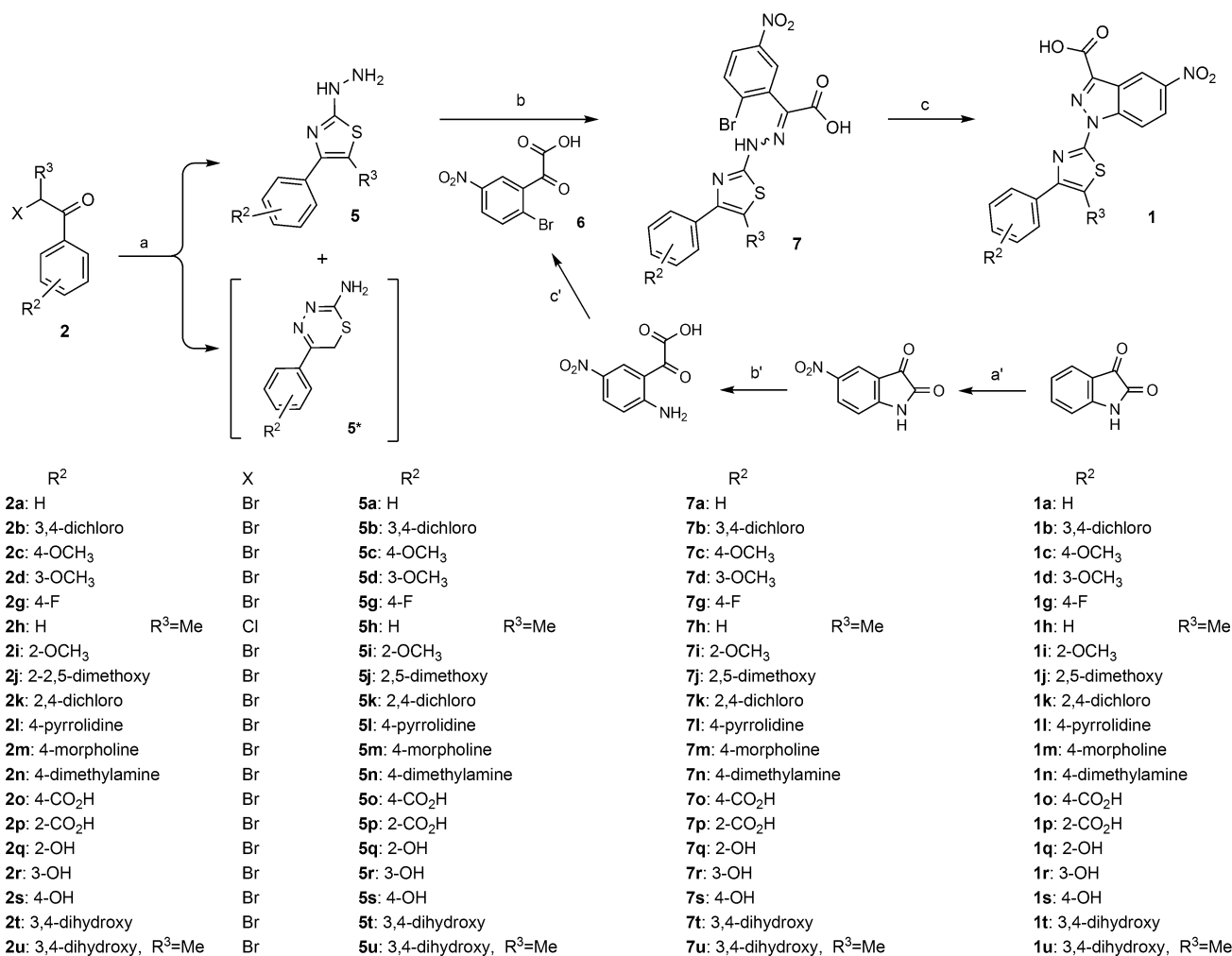
Scheme 5. Linear synthesis of 3-substituted indazoles as configurationally constrained 4EGI-1 mimetics through stepwise assembly of hydrazones followed by intramolecular cyclization of these linear precursors to form the anticipated products. Reagents and conditions: a) thiosemicarbazide (1 equiv), 1,4-dioxane, RT, overnight; b) **6** (1 equiv), ethanol/water/acetic acid (10:4.5:0.5, v/v/v), reflux, overnight; c) CuI (0.1 equiv), DMEDA (0.3 equiv), Na$_2$CO$_3$ (2.2 equiv), ethanol/water (1:1, v/v); a′) NaNO$_3$/H$_2$SO$_4$, 0 °C;[39] b′) KOH at RT;[40] c′) i: NaNO$_2$/HBr at 0 °C, ii: CuBr/HBr(aq) at RT.

	R^2	X		R^2		R^2		R^2
2a:	H	Br	**5a**:	H	**7a**:	H	**1a**:	H
2b:	3,4-dichloro	Br	**5b**:	3,4-dichloro	**7b**:	3,4-dichloro	**1b**:	3,4-dichloro
2c:	4-OCH$_3$	Br	**5c**:	4-OCH$_3$	**7c**:	4-OCH$_3$	**1c**:	4-OCH$_3$
2d:	3-OCH$_3$	Br	**5d**:	3-OCH$_3$	**7d**:	3-OCH$_3$	**1d**:	3-OCH$_3$
2g:	4-F	Br	**5g**:	4-F	**7g**:	4-F	**1g**:	4-F
2h:	H, R^3=Me	Cl	**5h**:	H, R^3=Me	**7h**:	H, R^3=Me	**1h**:	H, R^3=Me
2i:	2-OCH$_3$	Br	**5i**:	2-OCH$_3$	**7i**:	2-OCH$_3$	**1i**:	2-OCH$_3$
2j:	2-2,5-dimethoxy	Br	**5j**:	2,5-dimethoxy	**7j**:	2,5-dimethoxy	**1j**:	2,5-dimethoxy
2k:	2,4-dichloro	Br	**5k**:	2,4-dichloro	**7k**:	2,4-dichloro	**1k**:	2,4-dichloro
2l:	4-pyrrolidine	Br	**5l**:	4-pyrrolidine	**7l**:	4-pyrrolidine	**1l**:	4-pyrrolidine
2m:	4-morpholine	Br	**5m**:	4-morpholine	**7m**:	4-morpholine	**1m**:	4-morpholine
2n:	4-dimethylamine	Br	**5n**:	4-dimethylamine	**7n**:	4-dimethylamine	**1n**:	4-dimethylamine
2o:	4-CO$_2$H	Br	**5o**:	4-CO$_2$H	**7o**:	4-CO$_2$H	**1o**:	4-CO$_2$H
2p:	2-CO$_2$H	Br	**5p**:	2-CO$_2$H	**7p**:	2-CO$_2$H	**1p**:	2-CO$_2$H
2q:	2-OH	Br	**5q**:	2-OH	**7q**:	2-OH	**1q**:	2-OH
2r:	3-OH	Br	**5r**:	3-OH	**7r**:	3-OH	**1r**:	3-OH
2s:	4-OH	Br	**5s**:	4-OH	**7s**:	4-OH	**1s**:	4-OH
2t:	3,4-dihydroxy	Br	**5t**:	3,4-dihydroxy	**7t**:	3,4-dihydroxy	**1t**:	3,4-dihydroxy
2u:	3,4-dihydroxy, R^3=Me	Br	**5u**:	3,4-dihydroxy, R^3=Me	**7u**:	3,4-dihydroxy, R^3=Me	**1u**:	3,4-dihydroxy, R^3=Me

1′ **a–c** had good solubility in methanol and DMSO at room temperature, their nitrated homologues **1a–c** became poorly soluble. The nitro group is an integral part of the 4EGI-1 pharmacophore and contributes to the activity of its indazole-derived mimetics (vide infra). In order to increase the solubilities of the 5-nitroindazole derivatives, we introduced polar groups on the phenylthiazolyl moiety. As expected, substituting the phenyl ring with polar groups such as hydroxy, carboxy, or amine groups resulted in improved solubilities of up to 32-fold. An improvement in DMSO solubility at room temperature was observed, for example, on going from **1a** (3.125 mm), the undecorated indazole-based constrained 4EGI-1 mimetic, to **1c** (50 mm), and to **1t** (100 mm). Notably, introduction of a methyl group at C-5 of the thiazole ring was also accompanied by improved solubility, as demonstrated by comparison of the non-methylated analogue **1a** (3.125 mm) with the methylated **1h** (37.5 mm). The better solubility of **1h** relative to **1a** suggests that steric hindrance introduced by C-5 methylation might prevent facile aggregation and nucleation, which could accelerate precipitation.[42]

Biology

The newly synthesized indazole-based constrained 4EGI-1 mimetic library **1** was evaluated in a cell-free fluorescent polarization (FP) eIF4E/eIF4G interaction assay. This assay reports on the ability of a small molecule to disrupt the interaction of a fluorescent-labeled eIF4G-derived peptide, containing the eIF4E-binding consensus sequence, with eIF4E,[20a] a proxy for disruption of the eIF4F complex. We chose a set of compounds (**1a**, **1d**, and **1l**) for further evaluation of their activity in cell-based secondary mechanistic assays: expression of oncogenic proteins encoded by weak mRNAs and disruption of endogenous eIF4E/eIF4G interaction in intact cells. Finally, we determined the cell proliferation inhibitory activities of these selected compounds to serve as a reporter of a global activity that might be based on their on-target and off-target activities.

Competitive inhibition of the eIF4E/eIF4G interaction by the constrained 4EGI-1 analogues: We have previously reported on using the same FP assay for the discovery and development of small molecules that disrupt eIF4E/eIF4G interactions.[20a] Briefly, we synthesized a fluorescein-tagged eIF4G-derived peptide that acts as a surrogate to the endogenous eIF4G. The synthetic fluorescent peptide contains the consensus eIF4E-binding motif Y(X)$_4$LΦ. We also generated the recombinant glutathione-S-transferase-tagged fusion protein GST-DN26-eIF4E (in which eIF4E was truncated by the first N-terminal 26 amino acids). Here, (Z)-4EGI-1 was used in the FP assay as a positive control and the vehicle (DMSO) as a negative control. We report the potencies of the new indazole-based constrained 4EGI-1 mimetics **1** as ratios between the IC$_{50}$ of the (Z)-4EGI-1 and the IC$_{50}$ values of compounds **1** (Table 1).
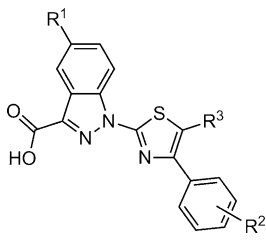
The locking of the (E)-4EGI-1 geometry in the corresponding indazole-based mimetic **1b** resulted in a significant increase in relative binding affinity [cf. IC$_{50}$ (Z)-4EGI-1/IC$_{50}$ (E)-4EGI-1 = 0.84 to IC$_{50}$ (Z)-4EGI-1/IC$_{50}$ **1b** = 1.40; Entries 1 and 7 in Table 1]. Evidently, locking the hit compound 4EGI-1 in the *E*-mimicking configuration, as in the indazole system, is either neutral or enhances the affinity for eIF4E, relative to either the *E* or the *Z* isomers of 4EGI-1. This result was encouraging and suggested that the indazole scaffold is a constrained chemotype that mimics 4EGI-1 in inhibiting eIF4E/eIF4G interaction. Compounds **1a–u** exhibit a range of competitive binding affinities that vary from no activity to four-times-higher affinity than (Z)-4EGI-1 (Table 1). Comparison of the relative competitive binding affinities of **1′a–c** with those of **1a–c** highlights the notable contribution of the 5-NO$_2$ group to the binding affinities of these nitrated derivatives to eIF4E. Previous SAR studies conducted in our laboratory found that the *ortho*-nitro group on the phenylpyruvic acid moiety of 4EGI-1 was itself an indispensable feature of the minimal pharmacophore.

The substituent at the *para* position of the 4-phenylthiazolyl moiety plays an important role in the interaction of the indazole-derived ligands with eIF4E. Whereas 4-chloro-, 4-fluoro-, and 2,4-difluorophenyl substituents, as in **1e**, **1g**, and **1f**, respectively, are less potent than, or equipotent to, the hit 4EGI-1, the 2,4- and 3,4-dichlorophenyl substituents, as in derivatives **1k** and **1b**, respectively, are more potent than (Z)-4EGI-1. Diversifying the nature of the substituents at the *para* position of the 4-phenylthiazolyl moiety, to include polar and potentially charged ones, not only contributed to improved solubility but also generated some of the most potent competitive binders to eIF4E. The changes in the apparent binding affinities of the 2-, 3-, and 4-hydroxyphenyl- (**1q**, **1r**, and **1s**) and the 3,4-dihydroxyphenyl-substituted (**1t**) analogues exemplify the complex structure–activity relationship in this focused library. Whereas **1r**, the 3-hydroxy-substituted analogue, is less potent than 4EGI-1 and the 2-hydroxy- and 4-hydroxy-substituted analogues **1q** and **1s**, respectively, the 3,4-dihydroxy analogue **1t** and the 4-hydroxy analogue **1s** are the most potent analogues in this series [IC$_{50}$ (Z)-4EGI-1/IC$_{50}$ **1** = 4.09 and 4.12, respectively]. O-Methylation of the hydroxy groups affects the apparent binding affinities in a position-dependent manner: whereas O-methylation of the 2-OH and 3-OH analogues enhances relative binding affinity (cf. 1.02 for **1q** vs. 1.92 for **1i** and 0.75 for **1r** vs. 4.04 for **1d**), O-methylation of 4-OH results in significant loss of apparent binding affinity (4.12 for **1s** vs. 1.70 for **1c**). Interestingly, the apparent binding affinity of the 2,4-dimethoxy analogue is significantly lower than those of the 2-methoxy- and 4-methoxy-substituted analogues (cf. 1.05 for **1j** vs. 1.92 and 1.70 for **1i** and **1c**, respectively). Introduction of potentially positively charged disubstituted amines at the *para* position of the 4-phenylthiazolyl group enhances apparent binding affinity gradually from 4-dimethylamino to 4-morpholino and 4-pyrrolidino (1.81 for **1n**, 2.24 for **1m**, and 2.70 for **1l**). The position-dependency of the binding affinities is also underscored in the marked differences between the inactive 2-CO$_2$H-substituted and the potent 4-CO$_2$H-substituted derivatives **1p** and **1o**, respectively.

In summary, it is evident that apparent binding affinities of the constrained 4EGI-1 mimetics towards eIF4E are greatly affected by the natures and positions of the substituents on the

Table 1. Binding of the configurationally constrained indazole-based 4EGI-1 mimetics to eIF4E as measured by fluorescence polarization assay (FP).

	Compound	R^1	R^2	R^3	IC$_{50}$ (Z)-4EGI-1/IC$_{50}$ **1**[a]
1	(E)-4EGI-1	NO$_2$	3,4-dichloro	H	0.84 ± 0.07 (41.5)[b]
2	(Z)-4EGI-1	NO$_2$	3,4-dichloro	H	1.00 ± 0.00 (32.0)[b]
3	**1′a**	H	H	H	n.a.[c]
4	**1′b**	H	3,4-dichloro	H	n.a.[c]
5	**1′c**	H	4-OCH$_3$	H	0.40 ± 0.05
6	**1a**	NO$_2$	H	H	0.82 ± 0.01
7	**1b**	NO$_2$	3,4-dichloro	H	1.40 ± 0.11
8	**1c**	NO$_2$	4-OCH$_3$	H	1.70 ± 0.18
9	**1d**	NO$_2$	3-OCH$_3$	H	4.04 ± 0.52
10	**1e**	NO$_2$	4-Cl	H	0.91 ± 0.08
11	**1f**	NO$_2$	2,4-difluoro	H	0.98 ± 0.03
12	**1g**	NO$_2$	4-F	H	0.61 ± 0.06
13	**1h**	NO$_2$	H	Me	2.10 ± 0.14
14	**1i**	NO$_2$	2-OCH$_3$	H	1.92 ± 0.12
15	**1j**	NO$_2$	2,5-dimethoxy	H	1.05 ± 0.01
16	**1k**	NO$_2$	2,4-dichloro	H	2.61 ± 0.24
17	**1l**	NO$_2$	4-pyrrolidine	H	2.70 ± 0.12
18	**1m**	NO$_2$	4-morpholine	H	2.24 ± 0.05
19	**1n**	NO$_2$	4-N(Me)$_2$	H	1.81 ± 0.03
20	**1o**	NO$_2$	4-CO$_2$H	H	2.83 ± 0.07
21	**1p**	NO$_2$	2-CO$_2$H	H	n.a.[c]
22	**1q**	NO$_2$	2-OH	H	1.02 ± 0.03
23	**1r**	NO$_2$	3-OH	H	0.75 ± 0.01
24	**1s**	NO$_2$	4-OH	H	4.12 ± 0.40
25	**1t**	NO$_2$	3,4-dihydroxy	H	4.09 ± 0.12
26	**1u**	NO$_2$	3,4-dihydroxy	Me	2.26 ± 0.35

[a] The relative binding affinities of the library of compounds **1** as measured by their activities in the fluorescence polarization assay. The relative activity of (Z)-4EGI-1 is given as 1. [b] The values in brackets are the IC$_{50}$ values in μM. [c] Not active.

4-phenylthiazolyl moiety. We are greatly encouraged by the tolerance of polar and potentially charge-bearing substituents that could be important modifiers of physicochemical and pharmacokinetic properties.

Inhibition of eIF4E/eIF4G interaction in cells: Encouraged by the results of the cell-free FP assay, in which the indazole-based constrained (*E*)-4EGI-1 mimetics displayed high activities, we selected representative analogues from this series for target validation in cell-based assays. Inhibition of eIF4E/eIF4G PPI in CRL-2813 cells by **1d** was demonstrated in an eIF4E pull-down assay and compared with the case of (*E*)-4EGI-1 (Figure 1). Western blot analysis of cap-affinity pulled-down
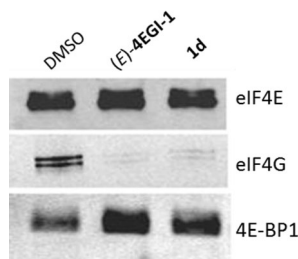

Figure 2. Inhibition of expression of oncogenic proteins by indazole-based constrained 4EGI-1 mimetics. Inhibition of the expression of oncogenes cyclin D1 and survivin in human melanoma CRL-2813 cells that had been treated with 4EGI-1 and indazole-based constrained 4EGI-1 mimetics at final concentrations of 50 and 25 μM for a time period of 8 h. Immunoblots for β-actin and GAPDH indicate equal loading and, as anticipated, lack of inhibition of expression for housekeeping proteins.

Figure 1. Compound **1d**, an indazole-based constrained mimetic of 4EGI-1, disrupts eIF4E/eIF4G interaction in a similar way to 4EGI-1. CRL-2813 human melanoma cells were treated with DMSO, (*E*)-4EGI-1, or compound **1d** at a final concentration of 50 μM for a time period of 8 h. Cell lysates were incubated with cap-conjugated agarose resin, and the retained material was eluted with m^7-GTP. The eluted material was separated by SDS-PAGE and immunoblotted with antibodies specific to eIF4E, eIF4G, and 4E-BP1.

material from lysates of melanoma cells treated variously with **1d**, (*E*)-4EGI-1, or vehicle (DMSO) revealed that treatment either with **1d** or with (*E*)-4EGI-1 depletes eIF4G from the eIF4E complex without any effect on the amount of eIF4E. As previously reported for 4EGI-1,[20a] here we also observed enhancement of 4E-BP1 binding in cells treated with (*E*)-4EGI-1 or **1d** relative to DMSO-treated cells (Figure 1).

Inhibition of oncogenic but not housekeeping protein expression: We anticipate that inhibition of translation initiation by disruption of eIF4F assembly should preferentially inhibit expression of growth-promoting, antiapoptotic, and oncogenic proteins, with minimal effect on the expression of housekeeping proteins. To validate this assumption, we treated CRL-2813 cells with the two indazole-based constrained 4EGI-1 mimetics **1a** and **1d** (these represent two levels of apparent binding affinity to eIF4E), as well as with 4EGI-1 and DMSO as positive and negative controls, respectively (Table 1). Indeed, like 4EGI-1, selected indazole-based compounds significantly inhibited the expression of survivin, an oncogenic protein that inhibits apoptosis and expression of cyclin D1, a promoter of G1/S cell cycle progression (Figure 2). Importantly, none of the indazole-based
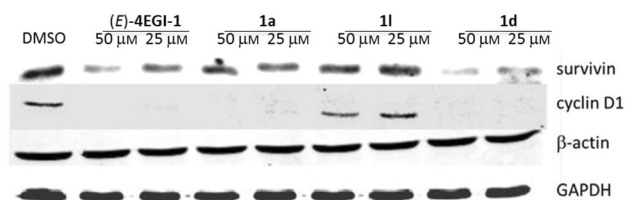
constrained 4EGI-1 mimetic analogues had any impact on the expression of β-actin or glyceraldehyde 3-phosphate dehydrogenase (GAPDH), two bona fide housekeeping proteins. Interestingly, compound **1l**, although active in the FP assay, does not appear to be active in the cell-based assays (see also Figure 4, below). This might be due variously to poor cell penetration, in vivo instability, or higher-affinity binding to other cellular proteins.

Inhibition of proliferation of cancer cells: Adherent human melanoma cells (CRL-2813), in addition to representing a prevalent human cancer, were found to be the most responsive to inhibition of proliferation by 4EGI-1.[20a] This sensitivity to antiproliferative agents is most likely attributable to the presence of a *BRAF* mutation.[43] We have previously shown that Ras-Raf-MAPK-driven cell proliferation is dependent on cyclin D1 expression.[44] The significant inhibition of cyclin D1 expression by our compounds might therefore explain, at least in part, the sensitivity of the melanoma cells to these agents. We therefore chose the CRL-2813 cells for evaluation of the antiproliferative activities of the three compounds—**1a**, **1d**, and **1l**—selected from the configurationally constrained (*E*)-4EGI-1 mimetic library (Table 2).

Table 2. *c* log *P* and IC$_{50}$ values [μM] of selected compounds from the library of the constrained mimetics of 4EGI-1 in inhibition of cell proliferation assay by SRB in human melanoma CRL-2813.

	Compound	R^1	R^2	R^3	*c* log *P*	SRB assay IC$_{50}$ in CRL-2813 [μM]
1	(*E*)-4EGI-1	NO$_2$	3,4-dichloro	H	4.76	1.23 ± 0.15
2	(*Z*)-4EGI-1	NO$_2$	3,4-dichloro	H	4.76	12.17 ± 0.95
3	**1a**	NO$_2$	H	H	3.99	5.65 ± 1.77
4	**1d**	NO$_2$	3-OCH$_3$	H	4.00	4.40 ± 0.57

Effects on regulators of the translation initiation machinery: We have previously shown that 4EGI-1 inhibits expression of mTOR and phosphorylation of 4E-BP1.[44] Similar inhibition of mTOR expression was observed with compound **1d**, as can be seen in Figure 3. Indazole derivative **1d** also inhibited p70S6K, a substrate for mTOR.

This finding prompted us to investigate the effects of selected indazole-based constrained 4EGI-1 mimetics on the expression and phosphorylation of 4E-BP1, downstream effector of
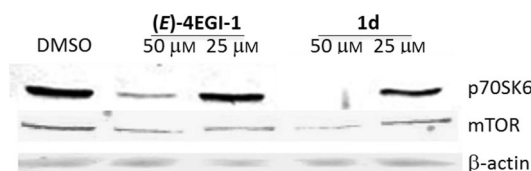
Figure 3. Effect of indazole-based constrained 4EGI-1 mimetic **1d** on the expression of mTOR. CRL-2813 were treated with DMSO, (E)-4EGI-1, or **1d** at final concentrations of 50 and 25 µm for a time period of 8 h, and lysates were immunoblotted with antibodies specific to mTOR and β-actin.

mTOR. Western blot analysis of CRL-2813 cell lysates treated with 4EGI-1, **1a**, **1l**, or **1d** shows that **1a** and **1d**, like 4EGI-1, reduced phosphorylation of 4E-BP1 (P-4E-BP1, Figure 4). Quan-
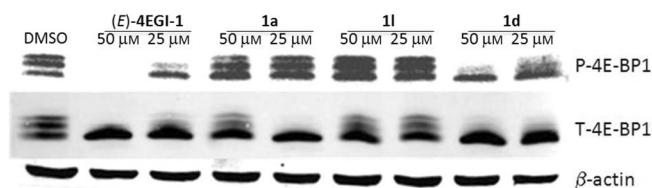

Figure 4. Effects of indazole-based constrained 4EGI-1 mimetics on the expression of downstream effectors of mTOR. CRL-2813 cells were treated with DMSO, (E)-4EGI-1, **1a**, **1l**, or **1d** at final concentrations of 50 and 25 µm for a time period of 8 h. Changes in the expression of p70S6K, phosphorylated- and total-4E-BP1 (P–4E-BP1 and T-4E-BP1, respectively) are shown. Immunoblotting for β-actin is shown as a control for total protein in the extract, and also as evidence for the lack of effect of these compounds on housekeeping proteins.

titative analysis of the ratio of phosphorylated 4E-BP1 (P-4E-BP1) to total 4E-BP1 (T-4E-BP1) indicates a significant effect for 4EGI-1 and **1d**, one of the most potent indazole-based constrained 4EGI-1 mimetics (Table 1), but a lesser effect for **1a**. Consistently with its modest effect on the expression of cyclin D1 or survivin (see Figure 2) compound **1l** had only a marginal effect on phosphorylation of 4E-BP1 (Figure 5). As anticipated, treatment with these agents did not affect expression of the housekeeping proteins β-actin and GAPDH. These data indicate that interfering with eIF4E/eIF4G PPI (Figure 1) inhibits translation initiation not only by blocking eIF4F formation but also by modifying expression of upstream mediators of phosphorylation of 4E-BP1 and p70S6K (Figures 4 and 6) perhaps in a feed-forward loop that further contributes to inhibition of translation initiation.

Effects of the constrained 4EGI-1 mimetics on protein expression are translational: To determine the mechanism of suppression of oncogenic protein expression by indazole-based constrained 4EGI-1 mimetics (Figures 4 and 6) we carried out real-time quantitative polymerase chain reaction (RT-PCR) analysis of the corresponding mRNAs with use of the 18S ribosomal RNA as an internal reference (Figure 6). Like 4EGI-1,
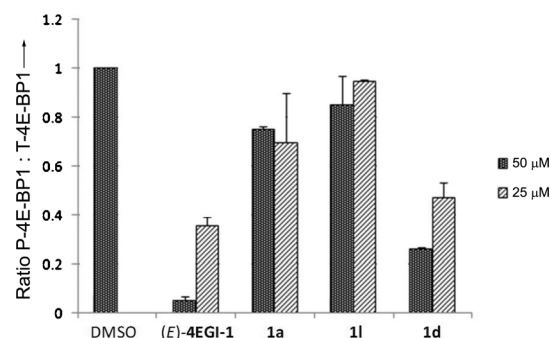

Figure 5. Effects of (E)-4EGI-1 and compounds **1a**, **1l**, and **1d** on the ratio of levels of phosphorylated 4E-BP1 (P-4E-BP1) to levels of total 4E-BP1 (T-4E-BP1) in CRL-2813, at final concentrations of 25 and 50 µm. Blots from two independent experiments were quantified with the aid of Odyssey software. The compounds reduced the levels of phosphorylated 4E-BP1 relative to the total amount.

the indazole-derived 4EGI-1 mimetics **1a** and **1d** did not reduce the levels of cyclin D1, survivin, and p70S6K mRNAs. We therefore conclude that inhibition of oncogenic protein expression by constrained 4EGI-1 derivatives is translational.

Conclusions

In light of the recent progress made in our understanding of the role of the eIF4F complex in normal biology and pathobiology, development of molecular probes that inhibit eIF4F complex formation is of great significance. Herein, we report a major advancement in the hit-to-lead optimization of 4EGI-1, the prototypic inhibitor of eIF4E/eIF4G interaction and cap-dependent translation initiation.[20a] We describe the rationale behind the design of the indazole-based constrained ana-
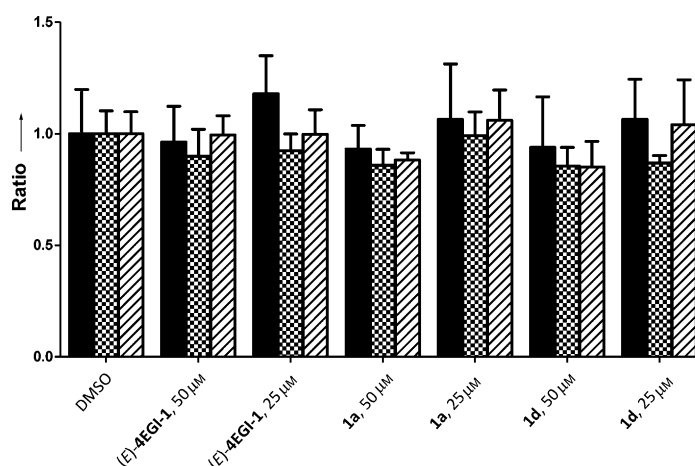

Figure 6. Effects of 4EGI-1 and its indazole-based constrained 4EGI-1 mimetics on mRNAs of cyclin D1, survivin, and p70S6K, expression of which was reduced in the presence of these analogues. Lysates of CRL-2813 cells that were incubated with the small molecules were analyzed by quantitative RT-PCR. The results from three independent experiments were calculated, and were then normalized to the levels of mRNA$_{18S}$. The data are shown as the means ± SDs and analyzed by use of one-way ANOVA with Dunnett post-test. The significance in difference was assigned at a level of less than a 5 % probability ($P < 0.05$). mRNA$_{cyclin\ D1}$/mRNA$_{18S}$ (solid bars), mRNA$_{survivin}$/mRNA$_{18S}$ (hashed bars), and mRNA$_{p70S6K}$/mRNA$_{18S}$ (diagonal stripe bars).

logues of the hit compound 4EGI-1, the development of an efficient synthetic pathway to obtain a focused library of such 3-substituted indazoles, and biological characterization of this library. In this new (E)-4EGI-1-mimetic chemotype, the original hydrazone moiety, which was susceptible to dynamic E-to-Z isomerization, becomes an integral part of the indazole scaffold and is locked in the E-mimicking configuration, prevented from isomerizing into the (Z)-4EGI-1-mimicking form. Our findings strongly suggest that the E configuration of 4EGI-1 contributes to the disruption of the interaction of eIF4E with eIF4G and to the inhibition of translation initiation. With this in mind, we demonstrate that structural rigidification can be combined with polarity- and solubility-enhancing substituents, resulting in molecular probes that avidly bind to eIF4E and effectively inhibit translation initiation. In summary, **1d** has emerged as a promising molecular probe for study of the role of eIF4F complexes in normal biology and pathobiology. We are continuing to explore a wide range of substituents on the phenyl rings and at position 5 of the thiazolidine ring in order to improve the potencies and bioavailabilities of these indazole-based 4EGI-1 mimetics further, with the intention of testing them as therapeutic agents in a variety of proliferative and neurodegenerative disorders. Furthermore, side-by-side comparison of these agents with chemical probes targeting other critical steps in the TI cascade[45] should shed light on the relative roles of various TI factors in normal biology and in pathobiology.

Experimental Section

Chemistry

General: Intermediates and final compounds were purified with a reversed-phase column (C18) and an Isolera flash chromatography system from Biotage, with use of a gradient of 0 to 100% methanol in water unless otherwise noted. Low-resolution HPLC-MS analysis was performed with a Waters Alliance-Micromass ZQ instrument, an ESI source, and an analytical Waters Symmetry C18 column (3.5 µm, 2.1×100 mm) operating at 0.5 mL min^{-1} with a linear gradient of 0–100% of acetonitrile in water (both solvents contain 0.1%, v/v, formic acid) over 10 min. The purities of the compounds were determined with a Waters Alliance analytical HPLC system operating at a flow rate of 1.0 mL min^{-1} and use of a linear gradient of 0–100% acetonitrile in water (both solvents contain 0.1%, v/v, trifluoroacetic acid) over 28 min on a Waters XBridge BEH 130 C18 column (5 µm, 4.6×100 mm). ^{1}H, ^{13}C, ^{19}F, and 2D NMR spectra were recorded at RT, unless otherwise noted, with a Varian Inova spectrophotometer (400 MHz for ^{1}H, 100 MHz for ^{13}C, and 376 MHz for ^{19}F) or a Varian Inova spectrophotometer (600 MHz for ^{1}H, 150 MHz for ^{13}C), as noted. Chemical shifts were referenced to the residual solvent peaks in the deuterated solvent used. HRMS spectra were measured with an Agilent 6210 Time-of-Flight LC-MS and ESI source; the differences between the measured ion masses and the expected ion masses were less than 5 ppm. Melting points were measured with an Electrothermal Mel-Temp manual melting point apparatus and are uncorrected.

General Procedure A—formation of thiocyanatoacetophenones 3a–h: The appropriate 2-bromoacetophenone derivative (10 mmol) was dissolved in acetonitrile (50 mL). Potassium thiocyanate (20 mmol) was added, and the mixture was heated at reflux for 2 h. The sol-

vents were removed under vacuum, and the residue was extracted with a mixture of ethyl acetate and water. The organic phase was dried (MgSO$_4$) and filtered, and the solvents were removed under vacuum to yield the pure product.

1-Phenyl-2-thiocyanatoethanone (3a): Off-white solid, 100% yield. M.p. 64°C; ^{1}H NMR (400 MHz, [D$_6$]DMSO): δ = 8.02 (d, J = 8.8 Hz, 2H), 7.72 (t, J = 7.2 Hz, 1H), 7.58 (t, J = 7.6 Hz, 2H), 5.11 ppm (s, 2H); ^{13}C NMR (100 MHz, [D$_6$]DMSO): δ = 192.8, 134.7, 129.4, 129.0, 113.3, 42.2 ppm; LC-MS (ESI+): m/z calcd for C$_9$H$_7$NOS: 177.02 [M+H]$^+$; found: 177.96.

1-(3,4-Dichlorophenyl)-2-thiocyanatoethanone (3b): Off-white solid, 100% yield. M.p. 103°C; ^{1}H NMR (400 MHz, [D$_6$]DMSO): δ = 8.25 (d, J = 2.0 Hz, 1H), 7.97 (dd, J = 8.4, 2.0 Hz, 1H), 7.52 (d, J = 8.4 Hz, 1H), 5.07 ppm (s, 2H); ^{13}C NMR (100 MHz, [D$_6$]DMSO): δ = 191.2, 137.5, 134.9, 132.5, 131.7, 131.0, 128.9, 113.0, 41.8 ppm; LC-MS (ESI+): m/z calcd for C$_9$H$_5$Cl$_2$NOS: 244.95 [M+H]$^+$; found: 245.85, 247.83.

1-(4-Methoxyphenyl)-2-thiocyanatoethanone (3c): White solid, 100% yield. M.p. 121°C; ^{1}H NMR (400 MHz, [D$_6$]DMSO): δ = 8.00 (d, J = 8.8 Hz, 2H), 7.09 (d, J = 8.8 Hz, 2H), 5.06 (s, 2H), 3.87 ppm (s, 3H); ^{13}C NMR (100 MHz, [D$_6$]DMSO): δ = 191.0, 164.5, 131.5, 127.6, 114.6, 113.4, 56.1, 42.1 ppm; LC-MS (ESI+): m/z calcd for C$_{10}$H$_9$NO$_2$S: 207.03 [M+H]$^+$; found: 207.98.

1-(3-Methoxyphenyl)-2-thiocyanatoethanone (3d): This compound was recrystallized from 95% ethanol to give yellow needles, 100% yield. M.p. 71°C; ^{1}H NMR (400 MHz, [D$_6$]DMSO): δ = 7.54 (d, J = 8.0 Hz, 1H), 7.47 (m, 2H), 7.27 (d, J = 8.0, 2.4 Hz, 1H), 5.08 (s, 2H), 3.82 ppm (s, 3H); ^{13}C NMR (100 MHz, [D$_6$]DMSO): δ = 192.6, 159.9, 136.1, 130.6, 121.5, 120.8, 113.5, 113.3, 55.9, 42.2 ppm; LC-MS (ESI+): m/z calcd for C$_{10}$H$_9$NO$_2$S: 207.03 [M+H]$^+$; found: 207.85; AHPLC: t_R = 13.36 min, 100%.

1-(4-Chlorophenyl)-2-thiocyanatoethanone (3e): White solid, 100% yield. M.p. 129°C; ^{1}H NMR (400 MHz, [D$_6$]DMSO): δ = 8.03 (d, J = 8.4 Hz, 2H), 7.66 (d, J = 8.8 Hz, 2H), 5.09 ppm (s, 2H); ^{13}C NMR (100 MHz, [D$_6$]DMSO): δ = 191.9, 139.7, 133.5, 131.0, 130.9, 129.6, 129.4, 113.2, 42.0 ppm; LC-MS (ESI+): m/z calcd for C$_9$H$_6$ClNOS: 210.99 [M+H]$^+$; found: 212.03.

1-(2,4-Difluorophenyl)-2-thiocyanatoethanone (3f): White solid, 100% yield. M.p. 64°C; ^{1}H NMR (400 MHz, [D$_6$]DMSO): δ = 8.04 (td, J = 8.8, 6.8 Hz, 1H), 7.50 (d, J = 11.6, 9.6, 2.4 Hz, 1H), 7.30 (dt, J = 8.8, 2.4 Hz, 1H), 4.96 ppm (d, J = 2.8 Hz, 1H); ^{13}C NMR (100 MHz, [D$_6$]DMSO): δ = 188.9 (d, J = 10.9, 3.9 Hz), 162.2 (dd, J = 269, 13.3 Hz), 162.8 (dd, J = 259, 13.2 Hz), 133.3, (dd, J = 10.9, 3.9 Hz), 120.3 (dd, J = 12, 4 Hz), 113.2 (d, J = 10.9 Hz), 113.1 (d, J = 21.8 Hz), 105.9 (t, J = 27 Hz), 45.0 ppm (d, J = 7.7 Hz); LC-MS (ESI−): m/z calcd for C$_9$H$_5$F$_2$NOS: 213.01 [M−H]$^-$; found: 212.09.

1-(4-Fluorophenyl)-2-thiocyanatoethanone (3g): White solid, 100% yield. M.p. 94°C; ^{1}H NMR (400 MHz, [D$_6$]DMSO): δ = 8.08 (dd, J = 8.6, 5.5 Hz, 2H), 7.39 (t, J = 8.8 Hz, 2H), 5.06 ppm (s, 2H); ^{13}C NMR (100 MHz, [D$_6$]DMSO): δ = 191.4 (d, J = 2.0 Hz), 167.3 (t, J = 6.0 Hz), 164.8, 133.0 (dd, J = 9.7, 5.8 Hz), 132.5 (d, J = 10.1 Hz), 131.9, 131.6 (m), 131.3 (dd, J = 9.7, 2.7 Hz), 117.3 (d, J = 22.5 Hz), 115.7 (d, J = 22.4 Hz), 113.2 (t, J = 4.7 Hz), 42.0 ppm; LC-MS (ESI+): m/z calcd for C$_9$H$_6$FNOS: 195.02 [M+H]$^+$; found: 196.03.

1-Phenyl-2-thiocyanatopropan-1-one (3h): Brown oil, 100% yield. ^{1}H NMR (400 MHz, [D$_6$]DMSO): δ = 8.05 (d, J = 7.2 Hz, 2H), 7.69 (d, J = 7.2 Hz, 1H), 7.56 (d, J = 7.6 Hz, 1H), 5.42 (q, J = 6.4 Hz, 1H), 1.63 ppm (d, J = 6.4 Hz, 3H); ^{13}C NMR (100 MHz, [D$_6$]DMSO): δ = 195.1, 134.6, 133.9, 129.4, 129.3, 111.5, 46.3, 18.4 ppm; LC-MS (ESI+): m/z calcd for C$_{10}$H$_9$NOS: 191.04 [M+H]$^+$; found: 191.94.

General Procedure B—formation of 2-chloro-4-phenylthiazoles 4a–h (adopted from Merijanian et al.[32]): Gaseous HCl was bubbled into a solution of the appropriate 1-phenyl-2-thiocyanatoethanone **3** (10 mmol) in dry ether (100 mL) at 0 °C, until saturation. The suspension was left to warm spontaneously to RT and stirred overnight. The volatiles were removed under vacuum, and the residue was dissolved in dichloromethane and washed with a saturated solution of NaHCO₃. The organic phase was dried (MgSO₄) and filtered, and the solvents were removed under vacuum. The residue was recrystallized from 95% ethanol.

2-Chloro-4-phenylthiazole (4a): Off-white needles, 90% yield. M.p. 48 °C; ^{1}H NMR (400 MHz, [D$_6$]DMSO): δ = 8.12 (s, 1H), 7.91 (d, J = 7.2 Hz, 2H), 7.47 (t, J = 7.6 Hz, 1H), 7.39 ppm (t, J = 7.2 Hz, 1H); ^{13}C NMR (100 MHz, [D$_6$]DMSO): δ = 153.3, 151.1, 133.4, 129.4, 129.0, 126.2, 117.5 ppm; LC-MS (ESI+): m/z calcd for C$_9$H$_6$ClNS: 194.99 [M+H]$^+$; found: 195.91, 197.86.

2-Chloro-4-(3,4-dichlorophenyl)thiazole (4b): White needles, 72% yield. M.p. 96 °C; ^{1}H NMR (400 MHz, [D$_6$]DMSO): δ = 8.29 (s, 1H), 8.10 (d, J = 1.6 Hz, 1H), 7.86 (dd, J = 8.4, 2.0 Hz, 1H), 7.67 ppm (d, J = 8.4 Hz, 1H); ^{13}C NMR (100 MHz, [D$_6$]DMSO): δ = 151.6, 150.6, 133.8, 132.2, 131.5, 131.4, 127.8, 126.3, 119.5 ppm; LC-MS (ESI+): m/z calcd for C$_9$H$_4$Cl$_3$NS: 262.91 [M+H]$^+$; found: 263.83, 265.81, 267.79.

2-Bromo-4-(4-methoxyphenyl)thiazole (4c): White solid, 89% yield. M.p. 97 °C; ^{1}H NMR (400 MHz, [D$_6$]DMSO): δ = 7.98 (s, 1H), 7.85 (d, J = 8.8 Hz, 2H), 7.01 (d, J = 8.8 Hz, 2H), 3.81 ppm (s, 3H); ^{13}C NMR (100 MHz, [D$_6$]DMSO): δ = 160.0, 154.8, 136.1, 127.7, 126.2, 116.9, 114.7, 55.7 ppm; LC-MS (ESI+): m/z calcd for C$_{10}$H$_8$BrNOS: 268.95 [M+H]$^+$; found: 269.78, 271.83.

2-Chloro-4-(3-methoxyphenyl)thiazole (4d): White needles, 78% yield. M.p. 53 °C; ^{1}H NMR (400 MHz, [D$_6$]DMSO): δ = 8.11 (s, 1H), 7.46 (d, J = 7.6 Hz, 1H), 7.42 (d, J = 2.4 Hz, 1H), 7.33 (t, J = 8.0 Hz, 1H), 6.92 (dd, J = 8.0, 2.4 Hz, 1H), 3.79 ppm (s, 3H); ^{13}C NMR (100 MHz, [D$_6$]DMSO): δ = 160.1, 153.1, 150.9, 134.8, 130.5, 118.6, 117.8, 114.8, 111.5, 55.6 ppm; LC-MS (ESI+): m/z calcd for C$_{10}$H$_8$ClNOS: 225.00 [M+H]$^+$; found: 225.89, 227.87; AHPLC: t_R = 16.97 min, 100%.

2-Chloro-4-(4-chlorophenyl)thiazole (4e): White solid, 100% yield. M.p. 99 °C; ^{1}H NMR (400 MHz, [D$_6$]DMSO): δ = 8.18 (s, 1H), 7.93 (d, J = 8.0 Hz, 2H), 7.52 ppm (d, J = 8.8 Hz, 2H); ^{13}C NMR (100 MHz, [D$_6$]DMSO): δ = 152.0, 151.4, 133.6, 132.3, 129.4, 128.0, 118.3 ppm; LC-MS (ESI+): m/z calcd for C$_9$H$_5$Cl$_2$NS: 228.95 [M+H]$^+$; found: 229.92, 231.93.

2-Chloro-4-(2,4-difluorophenyl)thiazole (4f): White solid, 89% yield. M.p. 54 °C; ^{1}H NMR (400 MHz, [D$_6$]DMSO): δ = 8.04 (td, J = 8.8, 6.4 Hz, 1H), 7.95 (d, J = 2.8 Hz, 1H), 7.41 (ddd, J = 12.0, 9.6, 2.8 Hz, 1H), 7.21 ppm (tdd, J = 8.4, 2.8, 0.8 Hz, 1H); ^{13}C NMR (100 MHz, [D$_6$]DMSO): δ = 162.4 (dd, J = 248.3, 12.4 Hz), 159.9 (dd, J = 252.3, 12.4 Hz), 151.2, 146.2, 131.3 (dd, J = 9.3, 3.8 Hz), 125.5 (d, J = 13.1 Hz), 118.0 (dd, J = 10.9, 3.1 Hz), 112.6 (dd, J = 21.1, 3.1 Hz), 105.3 ppm (t, J = 10.3 Hz); ^{19}F NMR (376 MHz, [D$_6$]DMSO): δ = −109.4 (quintet, J = 8 Hz), −110.1 ppm (qd, J = 9, 2.6 Hz); LC-MS (ESI+): m/z calcd for C$_9$H$_4$ClF$_2$NS: 230.97 [M+H]$^+$; found: 231.93, 233.95.

2-Chloro-4-(4-fluorophenyl)thiazole (4g): White solid, 76% yield. M.p. 78 °C; ^{1}H NMR (400 MHz, [D$_6$]DMSO): δ = 8.06 (s, 1H), 7.91 (dd, J = 8.4, 5.4 Hz, 1H), 7.25 ppm (t, J = 8.8 Hz, 1H); ^{13}C NMR (400 MHz, [D$_6$]DMSO): δ = 162.9 (d, J = 245.9 Hz), 152.5, 151.5, 130.3 (d, J = 2.2 Hz), 128.7 (d, J = 8.0 Hz), 117.6, 116.5 ppm (d, J = 21.9 Hz); ^{19}F NMR (376 MHz, [D$_6$]DMSO): δ = −113.5 ppm (septet); LC-MS

(ESI+): m/z calcd for C$_9$H$_5$ClFNS: 212.98 [M+H]$^+$; found: 213.98, 216.0.

2-Chloro-5-methyl-4-phenylthiazole (4h): Colorless oil, 75% yield. ^{1}H NMR (400 MHz, [D$_6$]DMSO): δ = 7.63 (d, J = 8.0 Hz, 2H), 7.47 (t, J = 8.4 Hz, 2H), 7.40 (t, J = 8.0 Hz, 1H), 2.52 ppm (s, 3H); ^{13}C NMR (400 MHz, [D$_6$]DMSO): δ = 149.4, 146.5, 133.8, 131.6, 129.0, 128.8, 128.6, 128.4, 12.8 ppm; LC-MS (ESI+): m/z calcd for C$_{10}$H$_8$ClNS: 209.01 [M+H]$^+$; found: 210.01, 212.03.

General Procedure C—formation of N-substituted indazoles 1′a–c and N-substituted 5-nitroindazoles 1a–h: 1H-Indazole-3-carboxylic acid (1 mmol) or 5-nitro-1H-indazole-3-carboxylic acid[33] (1 mmol) in DMSO (3 mL) was added dropwise to a suspension of NaOH (2.5 equiv, fine powder) in DMSO (1 mL). After 5 min, a solution of the appropriate 2-halo-4-phenylthiazole **4a–g** or 2-chloro-5-methyl-4-phenylthiazole (**4h**, 1 mmol) in DMSO (2 mL) was added, and the reaction mixture was heated at 120 °C for three days. The solution was allowed to cool to RT, and the formed precipitate was filtered, then resuspended in water, neutralized with HCl (0.1 M), and filtered. See workup for each compound below. Note: once the nitro group was introduced at C-5 of the indazole ring, the solubilities of these derivatives were significantly reduced to the extent that recording ^{13}C NMR was not possible because the compounds precipitated from the hot solutions during the acquisition, sometimes even when the probe's temperature was kept at 65 °C. To run a ^{13}C NMR scan with a less concentrated sample would take longer than 13 h.

1-(4-Phenylthiazol-2-yl)-1H-indazole-3-carboxylic acid (1′a): White solid, 31% yield. M.p. 370 °C; ^{1}H NMR (400 MHz, [D$_6$]DMSO): δ = 8.63 (d, J = 8.0 Hz, 1H), 8.38 (d, J = 7.6 Hz, 1H), 8.06 (d, J = 7.2 Hz, 1H), 7.87 (s, 1H), 7.64 (t, J = 7.2 Hz, 1H), 7.49 (t, J = 7.6 Hz, 2H), 7.37 ppm (m, 2H); ^{13}C NMR (100 MHz, [D$_6$]DMSO): δ = 164.7, 162.2, 151.9, 149.2, 139.0, 134.3, 129.3, 129.0, 128.7, 126.2, 126.0, 124.7, 124.0, 113.5, 109.8 ppm; LC-MS (ESI+): m/z calcd for C$_{17}$H$_{11}$N$_3$O$_2$S: 321.06 [M+H]$^+$; found: 322.19; HRMS (ESI+): calcd for C$_{17}$H$_{12}$N$_3$O$_2$S: 322.06447; found: 322.06490 [M+H]$^+$, 344.04683 [M+Na]$^+$; AHPLC: t_R = 17.74 min, 96.3%.

5-Nitro-1-(4-phenylthiazol-2-yl)-1H-indazole-3-carboxylic acid (1a): This compound was recrystallized from acetic acid. White needles, 40% yield. M.p. 298 °C; ^{1}H NMR (400 MHz, [D$_6$]DMSO): δ = 8.98 (d, J = 1.6 Hz, 1H), 8.91 (d, J = 9.6 Hz, 1H), 8.52 (dd, J = 9.2, 2.4 Hz, 1H), 8.08 (s + d, 3H), 7.52 (t, J = 7.6 Hz, 2H), 7.43 ppm (t, J = 7.6 Hz, 1H); ^{13}C NMR (150 MHz, [D$_6$]DMSO, recorded at 65 °C): δ = 162.0, 160.7, 152.5, 145.3, 141.9, 141.0, 133.9, 129.3, 128.9, 126.4, 124.8, 124.3, 119.4, 115.6, 112.2 ppm; LC-MS (ESI+): m/z calcd for C$_{17}$H$_{10}$N$_4$O$_4$S: 366.04 [M+H]$^+$; found: 366.95; HRMS (ESI+): calcd for C$_{17}$H$_{11}$N$_4$O$_4$S: 367.04955; found: 367.04880 [M+H]$^+$, 389.03101 [M+Na]$^+$; AHPLC: t_R = 17.83 min, 100%.

1-[4-(3,4-Dichlorophenyl)thiazol-2-yl]-1H-indazole-3-carboxylic acid (1′b): White solid, 21% yield. M.p. 289 °C; ^{1}H NMR (400 MHz, [D$_6$]DMSO): δ = 13.92 (br s, 1H), 8.66 (d, J = 8.4 Hz, 1H), 8.23 (d, J = 2.0 Hz, 1H), 8.20 (d, J = 8.4 Hz, 1H), 8.16 (s, 1H), 8.02 (dd, J = 8.4, 2.0 Hz, 1H), 7.76 (t, J = 7.2 Hz, 1H), 7.72 (d, J = 7.2 Hz, 1H), 7.52 ppm (t, J = 7.6 Hz, 1H); ^{13}C NMR (100 MHz, [D$_6$]DMSO): δ = 162.8, 161.7, 149.6, 140.4, 139.2, 134.5, 132.2, 131.5, 131.2, 130.3, 127.8, 126.5, 125.8, 124.7, 122.8, 114.3, 113.4 ppm; LC-MS (ESI+): m/z calcd for C$_{17}$H$_9$Cl$_2$N$_3$O$_2$S: 388.98 [M+H]$^+$; found: 390.02, 392.00; HRMS (ESI+): calcd for C$_{17}$H$_{10}$Cl$_2$N$_3$O$_2$S: 389.98653; found: 389.98689 [M+H]$^+$, 411.96699 [M+Na]$^+$; AHPLC: t_R = 22.99 min, 99.22%.

1-[4-(3,4-Dichlorophenyl)thiazol-2-yl]-5-nitro-1H-indazole-3-carboxylic acid (1b): This compound was recrystallized from acetic acid. Yellow solid, 33.8% yield. M.p. 339°C (decomp.); ^{1}H NMR (400 MHz, [D$_6$]DMSO): $\delta = 9.23$ (d, $J = 2.0$ Hz, 1H), 8.73 (d, $J = 9.2$ Hz, 1H), 8.46 (dd, $J = 9.2$, 2.4 Hz, 1H), 8.29 (d, $J = 2.4$ Hz, 1H), 8.15 (s, 1H), 8.08 (dd, $J = 8.4$, 2.4 Hz, 1H), 7.74 ppm (d, $J = 8.4$ Hz, 1H); ^{13}C NMR (100 MHz, [D$_6$]DMSO): $\delta = 162.4$, 161.9, 151.5, 149.5, 144.0, 140.6, 134.6, 132.2, 131.6, 131.1, 127.9, 126.6, 125.9, 123.9, 121.8, 114.4, 113.1 ppm; LC-MS (ESI−): m/z calcd for C$_{17}$H$_8$Cl$_2$N$_4$O$_4$S: 433.96; found: 435.04, 433.13 [M−H]$^-$, 391.08, 389.10 [M−NO$_2$]$^-$; HRMS (ESI−): calcd for C$_{17}$H$_7$Cl$_2$N$_4$O$_4$S: 432.9571; found: 432.9558 [M−H]$^-$; AHPLC: $t_R = 20.62$ min, 98.93%.

1-[4-(3,4-Dichlorophenyl)thiazol-2-yl]-5-nitro-1H-indazole-3-carboxylic acid (1′c): This compound was recrystallized from acetic acid. White solid, 25% yield. M.p. 229°C; ^{1}H NMR (400 MHz, [D$_6$]DMSO): $\delta = 8.73$ (d, $J = 8.4$ Hz, 1H), 8.23 (d, $J = 8.0$ Hz, 1H), 7.99 (d, $J = 8.8$ Hz, 2H), 7.80 (s, 1H), 7.76 (t, $J = 7.2$ Hz, 1H), 7.52 (t, $J = 7.6$ Hz, 1H), 7.04 (d, $J = 8.8$ Hz, 2H), 3.81 ppm (s, 3H); ^{13}C NMR (150 MHz, [D$_6$]DMSO): $\delta = 161.4$, 159.7, 158.3, 150.5, 137.7, 128.5, 126.1, 125.3, 124.0, 123.1, 121.2, 113.1, 112.8, 107.4, 54.1 ppm; LC-MS (ESI+): m/z calcd for C$_{18}$H$_{13}$N$_3$O$_3$S: 351.07 [M+H]$^+$; found: 352.03; HRMS (ESI+): calcd for C$_{18}$H$_{14}$N$_3$O$_3$S: 352.07504; found: 352.07541 [M+H]$^+$, 374.05702 [M+Na]$^+$; AHPLC: $t_R = 17.17$ min, 96.41%.

1-[4-(4-Methoxyphenyl)thiazol-2-yl]-5-nitro-1H-indazole-3-carboxylic acid (1c): Yellow solid, 60% yield. M.p. 281°C; ^{1}H NMR (400 MHz, [D$_6$]DMSO): $\delta = 9.22$ (d, $J = 2.0$ Hz, 1H), 8.76 (d, $J = 9.6$ Hz, 1H), 8.46 (dd, $J = 9.2$, 2.4 Hz, 1H), 8.00 (d, $J = 8.8$ Hz, 2H), 7.80 (s, 1H), 7.05 (d, $J = 8.8$ Hz, 2H), 3.82 ppm (s, 3H); ^{13}C NMR (400 MHz, [D$_6$]DMSO): $\delta = 162.5$, 161.3, 152.0, 144.0, 140.6, 127.8, 126.9, 125.7, 123.8, 121.7, 114.7, 114.4, 108.8, 55.7 ppm; LC-MS (ESI+): m/z calcd for C$_{18}$H$_{13}$N$_4$O$_5$S: 396.05 [M+H]$^+$; found: 397.03; HRMS (ESI+): calcd for C$_{18}$H$_{13}$N$_4$O$_5$S: 397.06012; found: 397.06071 [M+H]$^+$, 419.04280 [M+Na]$^+$; AHPLC: $t_R = 17.53$ min, 98.23%.

1-[4-(3-Methoxyphenyl)thiazol-2-yl]-5-nitro-1H-indazole-3-carboxylic acid (1d): Off-white solid, 39% yield. M.p. 286°C; ^{1}H NMR (400 MHz, [D$_6$]DMSO): $\delta = 8.98$ (s, 1H), 8.87 (d, $J = 9.6$ Hz, 1H), 8.59 (d, $J = 10.0$ Hz, 1H), 8.09 (s, 1H), 7.64 (d, $J = 7.2$ Hz, 1H), 7.56 (s, 1H), 7.41 (t, $J = 8.4$ Hz, 1H), 6.98 (dd, $J = 8.0$, 2.0 Hz, 1H), 3.85 ppm (s, 3H); ^{13}C NMR (100 MHz, [D$_6$]DMSO): $\delta = 161.3$, 160.2, 151.9, 144.0, 140.6, 135.4, 130.5, 125.7, 124.0, 121.6, 118.8, 114.4, 114.3, 118.9, 111.4, 55.7 ppm; MS (ESI+): m/z calcd for C$_{18}$H$_{12}$N$_4$O$_5$S: 396.05 [M+H]$^+$; found: 397.08; HRMS (ESI+): calcd for C$_{18}$H$_{13}$N$_4$O$_5$S: 397.06012; found: 397.05951; AHPLC: $t_R = 17.59$ min, 97.64%.

1-[4-(4-Chlorophenyl)thiazol-2-yl]-5-nitro-1H-indazole-3-carboxylic acid (1e): This compound was recrystallized from DMSO. Yellow solid, 33% yield. M.p. 348°C (decomp.); ^{1}H NMR (400 MHz, [D$_6$]DMSO): $\delta = 8.97$ (s, 1H), 8.87 (d, $J = 8.8$ Hz, 1H), 8.54 (dd, $J = 9.2$, 2.0 Hz, 1H), 8.11 (s, 1H), 8.08 (d, $J = 8.8$ Hz, 1H), 7.54 ppm (d, $J = 8.4$ Hz, 2H); LC-MS (ESI+): m/z calcd for C$_{17}$H$_9$ClN$_4$O$_4$S: 400.00 [M+H]$^+$; found: 401.07, 403.09; HRMS (ESI−): calcd for C$_{17}$H$_8$ClN$_4$O$_4$S: 398.9960 [M−H]$^-$; found: 398.9962; AHPLC: $t_R = 19.39$ min, 98.63%.

1-[4-(2,4-Difluorophenyl)thiazol-2-yl]-5-nitro-1H-indazole-3-carboxylic acid (1f): This compound was recrystallized from acetic acid. Yellow solid, 28% yield. M.p. 299°C; ^{1}H NMR (400 MHz, [D$_6$]DMSO): $\delta = 8.98$ (s, 1H), 8.79 (d, $J = 8.8$ Hz, 1H), 8.50 (d, $J = 8.4$ Hz, 1H), 8.23 (m, 1H), 7.84 (s, 1H), 7.35 (t, $J = 9.6$ Hz, 1H), 7.22 ppm (m, 1H); LC-MS (ESI+): m/z calcd for C$_{17}$H$_8$F$_2$N$_4$O$_4$S: 402.02 [M+H]$^+$; found: 402.96; HRMS (ESI−): calcd for C$_{17}$H$_7$F$_2$N$_4$O$_4$S: 401.0162 [M−H]$^-$; found: 401.0151; AHPLC: $t_R = 18.55$ min, 99.27%.

1-[4-(4-Fluorophenyl)thiazol-2-yl]-5-nitro-1H-indazole-3-carboxylic acid (1g): The reaction mixture was neutralized with HCl (1 N), and the precipitate was filtered, washed with water, and dried. Off-white solid, 100% yield. M.p. 309°C; ^{1}H NMR (400 MHz, [D$_6$]DMSO): $\delta = 9.27$ (d, $J = 2.4$ Hz, 1H), 8.78 (d, $J = 9.6$ Hz, 1H), 8.46 (dd, $J = 9.2$, 2.0 Hz, 1H), 8.15 (dd, $J = 8.4$, 5.2 Hz, 2H), 7.96 (s, 1H), 7.35 ppm (t, $J = 8.8$ Hz, 2H); ^{13}C NMR (100 MHz, [D$_6$]DMSO, recorded at 70°C): $\delta = 164.4$ (d, $J = 244.5$ Hz), 160.1, 150.6, 144.4, 140.3, 129.8, 127.8 (d, $J = 8.5$ Hz), 123.8, 118.9, 115.4, (d, $J = 21.0$ Hz), 114.7, 111.1 ppm; ^{19}F NMR (376 MHz, [D$_6$]DMSO): $\delta = -113.29$ ppm (m); LC-MS (ESI+): m/z calcd for C$_{17}$H$_9$FN$_4$O$_4$S: 384.03; found: 384.88 [M+H]$^+$, 366.90 [M−NO$_2$]$^+$; HRMS (ESI−): calcd for C$_{17}$H$_8$FN$_4$O$_4$S: 383.0256 [M−H]$^-$; found: 383.0251; AHPLC: $t_R = 17.94$ min, 100%.

1-(5-Methyl-4-phenylthiazol-2-yl)-5-nitro-1H-indazole-3-carboxylic acid (1h): White solid, 98% yield. M.p. 304°C (decomp.); ^{1}H NMR (400 MHz, [D$_6$]DMSO): $\delta = 9.26$ (d, $J = 1.6$ Hz, 1H), 8.64 (d, $J = 9.2$ Hz, 1H), 8.43 (dd, $J = 9.2$, 2.0 Hz, 1H), 7.82 (d, $J = 7.6$ Hz, 2H), 7.54 (t, $J = 7.6$ Hz, 2H), 7.44 (m, 1H), 2.61 ppm (s, 3H); LC-MS (ESI+): m/z calcd for C$_{18}$H$_{12}$N$_4$O$_4$S: 380.06 [M+H]$^+$; found: 381.10; HRMS (ESI+): calcd for C$_{18}$H$_{13}$N$_4$O$_4$S: 381.06520 [M+H]$^+$; found: 381.06635; AHPLC: $t_R = 18.84$ min, 100%.

General Procedure D—formation of 2-hydrazinyl-4-phenylthiazoles 5 and 5-phenyl-6H-1,3,4-thiadiazin-2-amines 5*: Thiosemicarbazide (1 mmol) was added to a solution of the appropriate bromoaceto-phenone (1 mmol) in dioxane (15 mL), and the mixture was stirred at RT overnight. For some of the derivatives, in addition to the desired 2-hydrazinyl-4-phenylthiazole 5, a six-membered isomer 5* was also formed. In some of these cases, the precipitate was filtered, dissolved in DMSO, and loaded on a RP-Biotage column. A linear gradient of 0–100% methanol in water was then used to allow the separation of the two isomers. Otherwise, the mixture of the isomers was used in the next step, in which the six-membered ring isomer remained unreacted. Additional workup, NMR data, LC-MS spectra, yields (for 5* yields are based on LCMS chromatograms), and melting points are given below for the 2-hydrazinyl-4-phenylthiazole derivatives 5 and in some cases for compounds 5* as well.

2-Hydrazinyl-4-phenylthiazole (5a): Brown solid, 27% yield. M.p. 129°C; ^{1}H NMR (400 MHz, [D$_6$]DMSO): $\delta = 8.55$ (s, 1H), 7.80 (d, $J = 8.2$ Hz, 2H), 7.36 (t, $J = 7.8$ Hz, 2H), 7.25 (t, $J = 7.2$ Hz, 1H), 7.09 (s, 1H), 4.85 ppm (br s, 2H); ^{13}C NMR (100 MHz, [D$_6$]DMSO): $\delta = 176.4$, 151.1, 135.7, 128.9, 127.6, 125.8, 102.3 ppm; LC-MS (ESI+): m/z calcd for C$_9$H$_9$N$_3$S: 191.05; found: 192.12 [M+H]$^+$, 175.07 [M−NH$_2$]$^+$; AHPLC: $t_R = 7.88$ min, 98.01%.

5-Phenyl-6H-1,3,4-thiadiazin-2-amine (5*a): Brown solid, 40% yield. M.p. 125°C; ^{1}H NMR (400 MHz, [D$_6$]DMSO): $\delta = 10.08$ (br s, 1H), 9.27 (br s, 1H), 7.85 (d, $J = 6.2$ Hz, 2H), 7.50 (m, 3H), 4.27 ppm (s, 2H); ^{13}C NMR (100 MHz, [D$_6$]DMSO): $\delta = 164.7$, 151.8, 133.4, 131.9, 129.5, 127.4, 22.6 ppm; LC-MS (ESI+): calcd for C$_9$H$_9$N$_3$S: 191.25 [M+H]$^+$; found: 192.12; AHPLC: $t_R = 7.38$ min, 98.92%.

4-(3,4-Dichlorophenyl)-2-hydrazinylthiazole (5b):[20a] Yellow solid, 80% yield. M.p. 107°C.

2-Hydrazinyl-4-(4-methoxyphenyl)thiazole (5c): Brown solid, 87% yield. M.p. 188°C; ^{1}H NMR (400 MHz, [D$_6$]DMSO): $\delta = 8.48$ (s, 1H), 7.70 (d, $J = 6.4$ Hz, 2H), 6.90 (d+s, 3H), 4.81 (s, 2H), 3.74 ppm (s, 3H); ^{13}C NMR (100 MHz, [D$_6$]DMSO): $\delta = 176.3$, 158.9, 150.9, 128.6, 127.2, 114.2, 100.3, 55.5 ppm; LC-MS (ESI+): m/z calcd for C$_{10}$H$_{11}$N$_3$OS: 221.06; found: 222.26 [M+H]$^+$, 205.20 [M−NH$_2$]$^+$; AHPLC: $t_R = 8.38$ min, 97.46%.

2-Hydrazinyl-4-(3-methoxyphenyl)thiazole (5d): Off-white solid, 44% yield. M.p. 140 °C; ^{1}H NMR (400 MHz, [D$_6$]DMSO): $\delta = 8.57$ (br s, 1H), 7.36 (m, 2H), 7.26 (t, $J = 8.0$ Hz, 1H), 7.11 (s, 1H), 6.82 (d, $J = 8.0$ Hz, 1H), 4.85 (br s, 2H), 3.77 ppm (s, 3H); ^{13}C NMR (100 MHz, [D$_6$]DMSO): $\delta = 181.0, 164.6, 155.7, 141.8, 134.7, 123.0, 118.0, 115.9, 107.6, 107.5, 60.2$ ppm; LC-MS (ESI+): m/z calcd for C$_{10}$H$_{11}$N$_3$OS: 221.06; found: 222.32 $[M+H]^+$, 206.27 $[M-NH]^+$; AHPLC: $t_R = 8.20$ min, 100%.

5-(3-Methoxyphenyl)-6H-1,3,4-thiadiazin-2-amine (5*d): Off-white solid, 16% yield. ^{1}H NMR (400 MHz, [D$_6$]DMSO): $\delta = 7.44$ (m, 3H), 7.13 (m, 1H), 4.29 (s, 2H), 3.80 ppm (s, 3H). ^{13}C NMR (100 MHz, [D$_6$]DMSO): $\delta = 164.7, 160.0, 151.6, 134.8, 130.7, 119.9, 117.8, 112.4, 55.9, 22.7$ ppm; LC-MS (ESI+): calcd for C$_{10}$H$_{11}$N$_3$OS: 221.28 $[M+H]^+$; found: 222.19; AHPLC: $t_R = 7.99$ min, 98.03%.

4-(4-Fluorophenyl)-2-hydrazinylthiazole (5g): Gray solid, 60% yield. M.p. 108 °C; ^{1}H NMR (400 MHz, [D$_6$]DMSO): $\delta = 8.57$ (s, 1H), 7.82 (d, $J = 5.6$ Hz, 2H), 7.15 (m, 2H), 7.03 (s, 1H), 4.86 ppm (s, 2H); ^{13}C NMR (100 MHz, [D$_6$]DMSO): $\delta = 176.7, 162.0$ (d, $J = 244.6$ Hz), 150.3, 132.5, 128.0 (d, $J = 8.0$ Hz), 115.9 (d, $J = 21.2$ Hz), 102.3 ppm; ^{19}F NMR (376 MHz, [D$_6$]DMSO): $\delta = -113.8$ ppm; LC-MS (ESI−): m/z calcd for C$_9$H$_8$FN$_3$S: 209.04 $[M-NH_2]^-$; found: 193.04; AHPLC: $t_R = 8.30$ min, 96.79%.

2-Hydrazinyl-5-methyl-4-phenylthiazole (5h): White solid, 66% yield. M.p. 155 °C; ^{1}H NMR (400 MHz, [D$_6$]DMSO): $\delta = 8.22$ (br s, 1H), 7.54 (d, $J = 8.8$ Hz, 2H), 7.36 (t, $J = 7.2$ Hz, 2H), 7.25 (m, 1H), 4.72 (br s, 2H), 2.33 ppm (s, 3H); ^{13}C NMR (100 MHz, [D$_6$]DMSO): $\delta = 172.3, 146.0, 136.3, 128.5, 128.2, 127.1, 115.6, 12.7$ ppm; LC-MS (ESI+): m/z calcd for C$_{10}$H$_{11}$N$_3$S: 205.07; found: 206.06 $[M+H]^+$, 189.01 $[M-NH_2]^+$; AHPLC: $t_R = 8.78$ min, 100%.

2-Hydrazinyl-4-(2-methoxyphenyl)thiazole (5i): Off-white solid, 89% yield. M.p. 122 °C; ^{1}H NMR (400 MHz, [D$_6$]DMSO): $\delta = 8.43$ (s, 1H), 8.01 (dd, $J = 7.6, 1.6$ Hz, 1H), 7.23 (m, 1H), 7.21 (s, 1H), 7.05 (d, $J = 8.0$ Hz, 1H), 6.96 (t, $J = 7.6$ Hz, 1H), 4.80 (s, 1H), 3.88 ppm (s, 3H); ^{13}C NMR (100 MHz, [D$_6$]DMSO): $\delta = 174.5, 157.0, 146.9, 129.4, 128.4, 123.8, 120.7, 111.8, 106.7, 55.8$ ppm. LC-MS (ESI+): m/z calcd for C$_{10}$H$_{11}$N$_3$OS: 221.06; found: 222.19 $[M+H]^+$, 205.14 $[M-NH_2]^+$; AHPLC: $t_R = 8.39$ min, 100%.

4-(2,5-Dimethoxyphenyl)-2-hydrazinylthiazole (5j): Brown solid, 88% yield. M.p. 123 °C; ^{1}H NMR (400 MHz, [D$_6$]DMSO): $\delta = 8.45$ (s, 1H), 7.58 (d, $J = 3.2$ Hz, 1H), 7.24 (s, 1H), 6.96 (d, $J = 9.2$ Hz, 1H), 6.78 (dd, $J = 8.8, 3.2$ Hz, 1H), 4.79 (s, 2H), 3.81 (s, 3H), 3.70 ppm (s, 3H); ^{13}C NMR (100 MHz, [D$_6$]DMSO): $\delta = 174.8, 153.6, 151.6, 147.0, 124.8, 114.9, 113.5, 113.2, 107.4, 56.5, 56.0$ ppm; LC-MS (ESI+): m/z calcd for C$_{11}$H$_{13}$N$_3$O$_2$S: 251.07; found: 252.06 $[M+H]^+$, 235.08 $[M-NH_2]^+$; AHPLC: $t_R = 8.80$ min, 98.68%.

4-(2,4-Dichlorophenyl)-2-hydrazinylthiazole (5k): Peach-colored solid, 88% yield. M.p. 145 °C; ^{1}H NMR (400 MHz, [D$_6$]DMSO): $\delta = 8.59$ (s, 1H), 7.86 (d, $J = 8.4$ Hz, 1H), 7.60 (d, $J = 2.0$ Hz, 1H), 7.43 (dd, $J = 8.4, 2.0$ Hz, 1H), 7.18 (s, 1H), 4.87 ppm (s, 2H); ^{13}C NMR (100 MHz, [D$_6$]DMSO): $\delta = 175.5, 146.4, 132.9, 132.7, 132.4, 131.7, 130.1, 127.8, 107.9$ ppm; LC-MS (ESI+): m/z calcd for C$_9$H$_7$Cl$_2$N$_3$S: 258.97; found: 261.91, 259.93 $[M+H]^+$, 244.89, 242.88 $[M-NH_2]^+$; AHPLC: $t_R = ?10.51$ min, 100%.

5-(2,4-Dichlorophenyl)-6H-1,3,4-thiadiazin-2-amine (5*k): Off-white solid, 8% yield. M.p. 161 °C; ^{1}H NMR (400 MHz, [D$_6$]DMSO): $\delta = 7.72$ (d, $J = 1.6$ Hz, 1H), 7.53 (d, $J = 8.0$ Hz, 1H), 7.50 (dd, $J = 8.4, 1.6$ Hz, 1H), 6.94 (br s, 2H), 3.54 ppm (s, 2H); ^{13}C NMR (100 MHz, [D$_6$]DMSO): $\delta = 149.7, 146.7, 136.6, 134.7, 132.7, 129.6, 127.9, 24.8$ ppm; LCMS (ESI+): calcd for C$_9$H$_7$Cl$_2$N$_3$S: 260.14 $[M+H]^+$; found: 262.04, 260.06; AHPLC: $t_R = 9.97$ min, 100%.

2-Hydrazinyl-4-[4-(pyrrolidin-1-yl)phenyl]thiazole (5l): Yellow solid, 44% yield. M.p. 106 °C; ^{1}H NMR (400 MHz, [D$_6$]DMSO): $\delta = 9.44$ (s, 2H), 7.47 (d, $J = 8.4$ Hz, 2H), 6.74 (s, 1H), 6.61 (d, $J = 8.4$ Hz, 2H), 3.25 (m, 4H), 1.94 ppm (m, 4H); ^{13}C NMR (100 MHz, [D$_6$]DMSO): $\delta = 168.6, 148.5, 142.5, 130.6, 115.4, 112.1, 99.0, 48.1, 25.4$ ppm; LC-MS (ESI+): m/z calcd for C$_{13}$H$_{16}$N$_4$S: 260.11; found: 261.18 $[M+H]^+$, 244.20 $[M-NH]^+$; AHPLC: $t_R = 10.61$ min, 95.91%.

5-[4-(Pyrrolidin-1-yl)phenyl]-6H-1,3,4-thiadiazin-2-amine (5*l): Yellow solid, 21% yield. ^{1}H NMR (400 MHz, [D$_6$]DMSO): $\delta = 7.76$ (d, $J = 8.4$ Hz, 2H), 6.63 (d, $J = 8.4$ Hz, 2H), 4.24 (s, 2H), 3.31 (m, 4H), 1.97 ppm (m, 4H); ^{13}C NMR (100 MHz, [D$_6$]DMSO): $\delta = 163.9, 152.1, 150.2, 129.0, 112.0, 47.7, 25.4, 22.3$ ppm; LC-MS (ESI+): calcd for C$_{13}$H$_{16}$N$_4$S: 260.36 $[M+H]^+$; found: 261.12; AHPLC: $t_R = 9.33$ min, 98.95%.

4-[4-(2-Hydrazinylthiazol-4-yl)phenyl]morpholine (5m): Compound **5m** was synthesized from **2m**[46] as described in General Procedure D. Orange solid, 48% yield. M.p. 181 °C; ^{1}H NMR (400 MHz, [D$_6$]DMSO): $\delta = 7.66$ (d, $J = 8.8$ Hz, 2H), 6.91 (d, $J = 9.2$ Hz, 2H), 6.86 (s, 1H), 3.73 (m, 4H), 3.11 ppm (m, 4H); ^{13}C NMR (100 MHz, [D$_6$]DMSO): $\delta = 176.1, 151.2, 150.5, 127.0, 126.7, 115.2, 99.6, 66.5, 48.7$ ppm; LC-MS (ESI+): m/z calcd for C$_{13}$H$_{16}$N$_4$OS: 276.10; found: 277.09 $[M+H]^+$, 260.02 $[M-NH_2]^+$; AHPLC: $t_R = 7.51$ min, 89.85%.

5-(4-Morpholinophenyl)-6H-1,3,4-thiadiazin-2-amine (5*m): Brown powder, 19% yield. M.p. 147 °C; ^{1}H NMR (400 MHz, [D$_6$]DMSO): $\delta = 7.77$ (d, $J = 8.8$ Hz, 2H), 6.98 (d, $J = 9.2$ Hz, 2H), 6.61 (br s, 2H), 3.74 (m, 4H), 3.59 (s, 2H), 3.19 ppm (m, 4H); ^{13}C NMR (100 MHz, [D$_6$]DMSO): $\delta = 152.4, 148.1, 128.0, 125.5, 114.6, 66.4, 48.0, 21.8$ ppm; LC-MS (ESI+): m/z calcd for C$_{13}$H$_{16}$N$_4$OS: 276.10 $[M+H]^+$; found: 277.03.

4-(2-Hydrazinylthiazol-4-yl)-N,N-dimethylaniline (5n): Compound **5n** was synthesized from **2n** [**2n** was formed by dimethylation[47] of 1-(4-aminophenyl)ethanone followed by bromination],[46] as described in General Procedure D. Brown solid, 74% yield. M.p. 165 °C; ^{1}H NMR (400 MHz, [D$_6$]DMSO): $\delta = 8.43$ (s, 1H), 7.61 (d, $J = 8.8$ Hz, 2H), 6.76 (s, 1H), 8.21 (d, $J = 8.8$ Hz, 2H), 4.80 (br s, 2H), 2.90 ppm (s, 6H); ^{13}C NMR (100 MHz, [D$_6$]DMSO): $\delta = 176.1, 151.7, 150.0, 126.8, 124.3, 112.5, 98.4$ ppm; LC-MS (ESI+): m/z calcd for C$_{11}$H$_{14}$N$_4$S: 234.09; found: 235.08 $[M+H]^+$, 218.03 $[M-NH_2]^+$.

4-(2-Hydrazinylthiazol-4-yl)benzoic acid (5o): Compound **5o** was synthesized from **2o**[46] as described in General Procedure D. Brown powder, 28% yield. M.p. 226 °C; ^{1}H NMR (400 MHz, [D$_6$]DMSO): $\delta = 8.65$ (s, 1H), 7.92 (m, 4H), 7.30 ppm (s, 1H); ^{13}C NMR (100 MHz, [D$_6$]DMSO): $\delta = 176.5, 167.6, 150.1, 149.6, 139.6, 130.1, 129.5, 125.8, 104.9$ ppm; LC-MS (ESI+): m/z calcd: 235.04; found: 236.00 $[M+H]^+$, 218.95 $[M-NH_2]^+$; AHPLC: $t_R = 6.37$ min, 95.88%.

4-(2-Amino-6H-1,3,4-thiadiazin-4-yl)benzoic acid (5*o): Brown powder, 50% yield. ^{1}H NMR (400 MHz, [D$_6$]DMSO): $\delta = 10.18$ (s, 1H), 9.37 (s, 1H), 8.00 (m, 4H), 4.32 ppm (s, 2H); ^{13}C NMR (100 MHz, [D$_6$]DMSO): $\delta = 167.1, 164.8, 150.8, 137.3, 133.4, 130.2, 127.6, 22.6$ ppm; LC-MS (ESI+): calcd for C$_{10}$H$_9$N$_3$O$_2$S: 235.26 $[M+H]^+$; found: 236.13; AHPLC: $t_R = 5.29$ min, 100%.

2-(2-Hydrazinylthiazol-4-yl)benzoic acid (5p): Compound **5p** was synthesized from **2p**,[48] as described in General Procedure D. Because of its fast degradation upon purification **5p** was used without purification. 21% yield. LC-MS (ESI+): m/z calcd for C$_9$H$_7$BrO$_3$: 235.04; found: 236.00 $[M+H]^+$, 217.96 $[M-NH_2]^+$.

2-(2-Hydrazinylthiazol-4-yl)phenol (5q): Compound **5q** was synthesized from **2q**[49] as described in General Procedure D. Off-white

solid, 32% yield. M.p. 190°C; ^{1}H NMR (400 MHz, [D$_6$]DMSO): $\delta =$ 11.84 (s, 1H), 8.91 (s, 1H), 7.62 (d, $J = 8.0$ Hz, 1H), 7.06 (m, 2H), 6.74 (m, 2H), 4.94 ppm (s, 2H); ^{13}C NMR (100 MHz, [D$_6$]DMSO): $\delta = 175.9$, 155.8, 148.7, 148.5, 129.3, 126.7, 119.3, 118.9, 117.3, 101.3 ppm; LC-MS (ESI+): m/z calcd for C$_9$H$_9$N$_3$OS: 207.05; found: 208.11 [M+H]$^+$, 191.06 [M−NH$_2$]$^+$; AHPLC: $t_R = 7.52$ min, 95.58%.

*2-(2-Amino-6H-1,3,4-thiadiazin-5-yl)phenol (5*q)*: Yellow solid, 62% yield. ^{1}H NMR (400 MHz, [D$_6$]DMSO): $\delta = 7.67$ (d, $J = 7.6$ Hz, 1H), 7.30 (t, $J = 7.6$ Hz, 1H), 7.17 (br s, 2H), 6.91 (m, 2H), 3.89 ppm (s, 2H); ^{13}C NMR (100 MHz, [D$_6$]DMSO): $\delta = 160.5$, 152.5, 151.9, 131.6, 128.1, 118.8, 117.6, 117.4, 20.5 ppm; LC-MS (ESI+): calcd for C$_9$H$_9$N$_3$OS: 207.25 [M+H]$^+$; found: 208.11; AHPLC: $t_R = 7.11$ min, 100%.

3-(2-Hydrazinylthiazol-4-yl)phenol (5r): Compound **5r** was synthesized from **2r**[49] as described in General Procedure D. Gray solid, 78% yield. M.p. 177°C; ^{1}H NMR (400 MHz, [D$_6$]DMSO): $\delta = 9.35$ (br s, 1H), 8.51 (s, 1H), 7.21 (m, 2H), 7.13 (t, $J = 8.0$ Hz, 1H), 6.99 (s, 1H), 6.65 (m, 1H), 4.83 ppm (br s, 2H); ^{13}C NMR (100 MHz, [D$_6$]DMSO): $\delta = 176.2$, 157.9, 151.2, 137.0, 129.8, 116.7, 114.6, 112.9, 102.2 ppm; LC-MS (ESI+): m/z calcd for C$_9$H$_9$N$_3$OS: 207.05; found: 208.05 [M+H]$^+$, 191.06 [M−NH$_2$]$^+$; AHPLC: $t_R = 6.59$ min, 93.38%.

4-(2-Hydrazinylthiazol-4-yl)phenol (5s): Compound **5s** was synthesized from **2s**[49] as described in General Procedure D. Yellow solid, 14% yield. M.p. 168°C; ^{1}H NMR (400 MHz, [D$_6$]DMSO): $\delta = 9.36$ (s, 1H), 8.37 (s, 1H), 7.53 (d, $J = 8.8$ Hz, 2H), 6.74 (s, 1H), 6.67 (d, $J = 8.8$ Hz, 2H), 4.73 ppm (s, 2H); ^{13}C NMR (100 MHz, [D$_6$]DMSO): $\delta = 176.1$, 157.2, 151.3, 127.2, 127.1, 115.6, 99.4 ppm; LC-MS (ESI+): m/z calcd for C$_9$H$_9$N$_3$OS: 207.05; found: 208.18 [M+H]$^+$, 191.19 [M−NH$_2$]$^+$; AHPLC: $t_R = 6.31$ min, 92.30%.

*4-(2-Amino-6H-1,3,4-thiadiazin-5-yl)phenol (5*s)*: Brown powder, 57% yield. ^{1}H NMR (400 MHz, [D$_6$]DMSO): $\delta = 7.66$ (d, $J = 8.8$ Hz, 2H), 6.75 (d, $J = 8.4$ Hz, 2H), 3.52 ppm (s, 2H); ^{13}C NMR (100 MHz, [D$_6$]DMSO): $\delta = 159.1$, 149.1, 147.1, 128.4, 127.3, 115.8, 21.9 ppm; LC-MS (ESI−): calcd for C$_9$H$_9$N$_3$OS: 207.25 [M−OH]$^-$; found: 190.20; AHPLC: $t_R = 9.66$ min, 96.60%.

4-(2-Hydrazinylthiazol-4-yl)benzene-1,2-diol (5t): Brown solid, 38% yield. M.p. 115°C; ^{1}H NMR (400 MHz, [D$_6$]DMSO): $\delta = 8.89$ (br s, 2H), 8.44 (s, 1H), 7.20 (d, $J = 2.4$ Hz, 1H), 7.06 (dd, $J = 8.0$, 2.0 Hz, 1H), 6.74 (s, 1H), 6.70 (d, $J = 8.0$ Hz, 1H), 2.54 ppm (s, 1H); ^{13}C NMR (400 MHz, [D$_6$]DMSO): $\delta = 175.9$, 151.5, 145.4, 145.3, 127.6, 117.3, 115.9, 113.7, 99.4 ppm; LC-MS (ESI−): m/z calcd for C$_9$H$_9$N$_3$O$_2$S: 223.04; found: 222.32 [M−H]$^-$, 206.26 [M−NH$_2$]$^-$; AHPLC: $t_R = 5.63$ min, 100%.

4-(2-Hydrazinyl-5-methylthiazol-4-yl)benzene-1,2-diol (5u): Compound **5u** was synthesized from **2u** and followed the General Procedure D (the synthesis of compound **2u**, from 2-bromopropanoic acid and resorcinol, was adopted from Koch et al.[50] generating an off-white solid, 82% yield. M.p. 151°C; ^{1}H NMR (400 MHz, [D$_6$]acetone): $\delta = 8.85$ (br s, 1H), 8.42 (s, 1H), 7.55 (m, 2H), 6.95 (d, $J = 8.8$ Hz, 1H), 5.56 (q, $J = 6.6$ Hz, 1H), 1.80 ppm (d, $J = 6.4$ Hz, 1H); ^{13}C NMR (100 MHz, [D$_6$]DMSO): $\delta = 182.4$, 141.6, 135.9, 117.4, 113.5, 106.5, 105.8, 32.8, 10.7 ppm; LC-MS (ESI+): m/z calcd for C$_9$H$_9$BrO$_3$: 243.97 [M+H]$^+$; found: 247.04, 244.99. Compound **5u** was obtained as a off-white solid, 74% yield. M.p. 154°C; ^{1}H NMR (400 MHz, [D$_6$]DMSO): $\delta = 9.02$ (br s, 2H), 7.03 (d, $J = 2.0$ Hz, 1H), 6.84 (dd, $J = 8.4$, 2.0 Hz, 1H), 6.77 (d, $J = 8.0$ Hz, 1H), 2.31 ppm (s, 3H); ^{13}C NMR (100 MHz, [D$_6$]DMSO): $\delta = 175.7$, 170.0, 145.3, 145.1, 126.6, 119.7, 116.1, 115.8, 113.9, 12.7 ppm; LC-MS (ESI+): m/z calcd for C$_{10}$H$_{11}$N$_3$O$_2$S: 237.06; found: 238.05 [M+H]$^+$, 221.00 [M−NH$_2$]$^+$.

5-Nitroisatine: This compound was prepared as described by Magiatis et al.[39] Orange solid, 100% yield. ^{1}H NMR (400 MHz, [D$_6$]DMSO): $\delta = 11.64$ (s, 1H), 8.41 (dd, $J = 8.8$, 2.4 Hz, 1H), 8.17 (d, $J = 2.4$ Hz, 1H), 7.06 ppm (d, $J = 8.8$ Hz, 1H); ^{13}C NMR (100 MHz, [D$_6$]DMSO): $\delta = 182.8$, 160.3, 155.6, 143.0, 133.5, 120.0, 118.5, 112.9 ppm; LC-MS (ESI−): m/z calcd for C$_8$H$_4$N$_2$O$_4$: 192.02; found: 190.86 [M−H]$^-$, 162.91 [M−CO]$^-$.

2-(2-Amino-5-nitrophenyl)-2-oxoacetic acid: This compound was prepared as described by Halváč et al.[39] ^{1}H NMR (400 MHz, [D$_6$]DMSO): $\delta = 8.39$ (d, $J = 2.8$ Hz, 1H of OH + 2H of NH$_2$), 8.11 (dd, $J = 9.2$, 2.4 Hz, 1H), 6.95 ppm (d, $J = 9.2$ Hz, 1H); ^{13}C NMR (100 MHz, [D$_6$]DMSO): $\delta = 189.7$, 166.0, 156.9, 135.6, 130.9, 130.4, 118.2, 110.3 ppm; LC-MS (ESI−): m/z calcd for C$_8$H$_6$N$_2$O$_5$: 210.03 [M−H]$^-$; found: 209.01.

2-(2-Bromo-5-nitrophenyl)-2-oxoacetic acid (6): The procedure was adopted from Pospíšil et al.[51] A solution of NaNO$_2$ (3.92 g, 56.8 mmol) in water (14 g) was added dropwise at 0°C to 2-(2-amino-5-nitrophenyl)-2-oxoacetic acid (5.0 g, 23.8 mmol) in aqueous HBr (14 mL of 48 wt.% in H$_2$O into 14 mL water) with maintenance of the temperature at 0°C. After the addition was complete, the solution was allowed to stir at this temperature for another 30 min and was then transferred slowly into a suspension of CuBr (6.2 g, 43.2 mmol) in aqueous HBr (14 mL of 48 wt.% in H$_2$O into 14 mL water). The resulting mixture was stirred at RT for an hour and then extracted with ethyl acetate. The organic phase was washed with saturated NaHCO$_3$ and brine, filtered through Celite, dried (MgSO$_4$), and concentrated to yield a yellow solid (82% yield). M.p. 109°C; ^{1}H NMR (400 MHz, [D$_6$]DMSO): $\delta = 8.49$ (d, $J = 2.8$ Hz, 1H), 8.27 (dd, $J = 8.4$, 2.8 Hz, 1H), 8.03 ppm (d, $J = 8.8$ Hz, 1H); ^{13}C NMR (100 MHz, [D$_6$]DMSO): $\delta = 187.5$, 162.1, 147.2, 138.4, 135.3, 127.9, 127.3, 125.9 ppm; LC-MS (ESI−): m/z calcd for C$_8$H$_4$BrNO$_5$: 272.93; found: 273.94, 271.96 [M−H]$^-$, 201.97, 199.92 [M−NO$_2$]$^-$; AHPLC: $t_R = 7.66$ min, 100%.

General Procedure E—formation of hydrazones 7: Compound **6** (2 mmol) and the appropriate 2-hydrazinyl-4-phenylthiazole (2 mmol) were heated at reflux for 3 h in a mixture of ethanol (10 mL), acetic acid (0.5 mL), and water (4.5 mL). The precipitate that formed was filtered; it was usually pure enough to be used in the next step. Otherwise, further purification was carried out by RP Biotage with a gradient of 0–100% methanol in water for 12 column volumes.

2-(2-Bromo-5-nitrophenyl)-2-[2-(4-phenylthiazol-2-yl)hydrazono]acetic acid (7a): Yellow solid, 91% yield. M.p. 216°C; ^{1}H NMR (400 MHz, [D$_6$]DMSO): $\delta = 8.28$ (s, 1H), 8.20 (dd, $J = 8.8$, 2.8 Hz, 1H), 8.02 (d, $J = 8.8$ Hz, 1H), 7.79 (d, $J = 7.6$ Hz, 2H), 7.46 (br s, 1H), 7.37 (m, 2H), 7.28 ppm (t, $J = 7.2$ Hz, 1H); ^{13}C NMR (100 MHz, [D$_6$]DMSO): $\delta = 164.2$, 147.7, 134.5, 130.9, 129.1, 126.8, 126.0, 125.9, 106.4 ppm; LC-MS (ESI+): m/z calcd for C$_{17}$H$_{11}$BrN$_4$O$_4$S: 445.97 [M+H]$^+$; found: 446.82, 448.88; AHPLC: $t_R = 15.33$ min, 96.27%.

2-(2-Bromo-5-nitrophenyl)-2-{2-[4-(3,4-dichlorophenyl)thiazol-2-yl]hydrazono}acetic acid (7b): Yellow solid, 52% yield. M.p. 209°C; ^{1}H NMR (400 MHz, [D$_6$]DMSO): $\delta = 8.29$ (d, $J = 2.8$ Hz, 1H), 8.21 (dd, $J = 8.8$, 2.4 Hz, 1H), 8.03 (m, 2H), 7.78 (dd, $J = 8.8$, 2.0 Hz, 1H), 7.69 (br s, 1H), 7.63 ppm (d, $J = 8.8$ Hz, 1H); ^{13}C NMR (100 MHz, [D$_6$]DMSO): $\delta = 164.0$, 147.7, 134.6, 131.9, 131.4, 130.9, 130.4, 127.7, 126.1, 126.9, 126.0 ppm; LC-MS (ESI+): m/z calcd for C$_{17}$H$_9$BrCl$_2$N$_4$O$_4$S: 513.89 [M+H]$^+$; found: 518.75, 516.70, 514.72; AHPLC: $t_R = 18.11$ min, 100%.

2-(2-Bromo-5-nitrophenyl)-2-{2-[4-(4-methoxyphenyl)thiazol-2-yl]hydrazono}acetic acid (7c): Yellow solid, 66% yield. M.p. 204°C;

^{1}H NMR (400 MHz, [D$_6$]DMSO): δ = 8.28 (d, J = 2.8 Hz, 1H), 8.21 (dd, J = 9.2, 2.8 Hz, 1H), 8.04 (d, J = 8.8 Hz, 1H), 7.73 (d, J = 8.8 Hz, 2H), 7.28 (s, 1H), 6.94 (d, J = 8.8 Hz, 2H), 3.77 ppm (s, 3H); ^{13}C NMR (100 MHz, [D$_6$]DMSO): δ = 164.2, 159.4, 147.7, 134.5, 131.0, 127.3, 126.8, 126.0, 114.5, 55.6 ppm; LC-MS (ESI+): m/z calcd for C$_{18}$H$_{13}$BrN$_4$O$_5$S: 475.98; found: 477.09, 479.14 [M+H]$^+$, 431.14, 433.13 [M−NO$_2$]$^+$; AHPLC: t_R = 15.11 min, 95.81%.

2-(2-Bromo-5-nitrophenyl)-2-{2-[4-(3-methoxyphenyl)thiazol-2-yl]hydrazono}acetic acid (7d): Light yellow solid, 84% yield. M.p. 197 °C; ^{1}H NMR (400 MHz, [D$_6$]DMSO): δ = 8.30 (d, J = 2.8 Hz, 1H), 8.22 (dd, J = 8.8, 2.8 Hz, 1H), 8.04 (d, J = 8.8 Hz, 1H), 8.02 (s, 1H), 7.50 (s, 1H), 7.34 (m, 2H), 7.29 (t, J = 7.6 Hz, 1H), 6.86 (dd, J = 8.4, 2.0 Hz, 1H), 3.76 ppm (s, 3H); ^{13}C NMR (100 MHz, [D$_6$]DMSO, 65 °C): δ = 164.0, 160.2, 147.9, 134.5, 130.8, 130.1, 126.9, 126.7, 125.8, 118.5, 114.3, 111.5, 55.7 ppm; LC-MS (ESI+): m/z calcd for C$_{18}$H$_{13}$BrN$_4$O$_5$S: 475.98 [M+H]$^+$; found: 476.96, 478.91; AHPLC: t_R = 15.30 min, 94.32%.

2-(2-Bromo-5-nitrophenyl)-2-{2-[4-(4-fluorophenyl)thiazol-2-yl]hydrazono}acetic acid (7g): Yellow solid, 96% yield. M.p. 220 °C; ^{1}H NMR (400 MHz, [D$_6$]DMSO): δ = 8.30 (d, J = 2.4 Hz, 1H), 8.22 (dd, J = 8.4, 2.8 Hz, 1H), 8.04 (d, J = 8.4 Hz, 1H), 7.84 (dd, J = 8.4, 5.6 Hz, 2H), 7.46 (s, 1H), 7.22 ppm (m, 2H); ^{13}C NMR (400 MHz, [D$_6$]DMSO): δ = 164.1, 162.2 (d, J = 245.1 Hz), 147.7, 134.5, 130.9, 128.0 (d, J = 7.7 Hz), 126.8, 126.0, 115.9 ppm (d, J = 21.8 Hz); LC-MS (ESI−): m/z calcd for C$_{17}$H$_{10}$BrFN$_4$O$_4$S: 463.96 [M−H]$^−$; found: 462.88, 464.90; AHPLC: t_R = 15.66 min, 100%.

2-(2-Bromo-5-nitrophenyl)-2-[2-(5-methyl-4-phenylthiazol-2-yl)hydrazono]acetic acid (7h): Yellow solid, 91% yield. M.p. 213 °C; ^{1}H NMR (400 MHz, [D$_6$]DMSO): δ = 8.21 (s, 1H), 8.16 (d, J = 7.6 Hz, 1H), 8.00 (d, J = 8.4 Hz, 1H), 7.52 (m, 2H), 7.39 (m, 2H), 7.31 (m, 1H), 2.39 ppm (s, 3H); ^{13}C NMR (100 MHz, [D$_6$]DMSO): δ = 164.4, 147.6, 134.4, 131.0, 128.8, 128.4, 128.0, 126.7, 125.7, 12.7 ppm; LC-MS (ESI+): m/z calcd for C$_{18}$H$_{13}$BrN$_4$O$_4$S: 459.98; found: 463.01, 461.03 [M+H]$^+$, 417.00, 415.01 [M−NO$_2$]$^+$; AHPLC: t_R = 15.43 min, 100%.

2-(2-Bromo-5-nitrophenyl)-2-{2-[4-(2-methoxyphenyl)thiazol-2-yl]hydrazono}acetic acid (7i): Yellow solid, 94% yield. M.p. 168 °C; ^{1}H NMR (400 MHz, [D$_6$]DMSO): δ = 8.26 (s, 1H), 8.19 (d, J = 8.8 Hz, 1H), 8.01 (d, J = 89.2 Hz, 1H), 7.89 (d, J = 7.2 Hz, 1H), 7.46, (s, 1H), 7.26 (t, J = 7.6 Hz, 1H), 7.08 (d, J = 8.4 Hz, 1H), 6.94 (t, J = 7.6 Hz, 1H), 3.88 pm (s, 3H); ^{13}C NMR (100 MHz, [D$_6$]DMSO): δ = 164.3, 157.0, 147.7, 134.5, 131.0, 129.3, 129.2, 126.8, 125.9, 120.8, 112.0, 55.9 ppm; LC-MS (ESI+): m/z calcd for C$_{18}$H$_{13}$BrN$_4$O$_5$S: 475.99 [M+H]$^+$; found: 477.09, 479.08; AHPLC: t_R = 15.41 min, 100%.

2-(2-Bromo-5-nitrophenyl)-2-{2-[4-(2,5-dimethoxyphenyl)thiazol-2-yl]hydrazono}acetic acid (7j): Yellow solid, 78% yield. M.p. 165 °C; ^{1}H NMR (400 MHz, [D$_6$]DMSO): δ = 8.25 (s, 1H), 8.19 (d, J = 8.4 Hz, 1H), 8.02 (d, J = 8.4 Hz, 1H), 7.51 (s, 1H), 7.49 (s, 1H), 7.00 (d, J = 9.2 Hz, 1H), 6.82 (d, J = 9.2, 2.4 Hz, 1H), 3.83 (s, 3H), 3.65 ppm (s, 3H); ^{13}C NMR (100 MHz, [D$_6$]DMSO): δ = 164.2, 153.4, 151.3, 147.7, 134.5, 131.0, 126.8, 125.9, 114.4, 114.1, 113.3, 56.3, 55.9 ppm; LC-MS (ESI+): m/z calcd for C$_{19}$H$_{15}$BrN$_4$O$_6$S: 505.99; found: 507.24, 509.16 [M+H]$^+$, 461.16, 463.21 [M−NO$_2$]$^+$; AHPLC: t_R = 15.49 min, 100%.

2-(2-Bromo-5-nitrophenyl)-2-{2-[4-(2,4-dichlorophenyl)thiazol-2-yl]hydrazono}acetic acid (7k): Light pink solid, 98% yield. M.p. 206 °C; ^{1}H NMR (400 MHz, [D$_6$]DMSO): δ = 8.31 (d, J = 2.8 Hz, 1H), 8.22 (dd, J = 9.2, 2.8 Hz, 1H), 8.04 (d, J = 8.8 Hz, 1H), 7.80 (d, J = 8.8 Hz, 1H), 7.68 (d, J = 2.0 Hz, 1H), 7.53(s, 1H), 7.47 ppm (dd, J = 8.8, 2.4 Hz, 1H); ^{13}C NMR (100 MHz, [D$_6$]DMSO): δ = 164.1, 147.7, 134.5, 133.3, 132.7, 132.2, 130.9, 130.2, 127.9, 126.8, 126.1 ppm; LC-MS (ESI+): m/z calcd for C$_{17}$H$_9$BrCl$_2$N$_4$O$_4$S: 513.89 [M+H]$^+$; found: 514.93, 516.95, 518.90; AHPLC: t_R = 18.06 min, 93.65%.

2-(2-Bromo-5-nitrophenyl)-2-(2-{4-[4-(pyrrolidin-1-yl)phenyl]thiazol-2-yl}hydrazono)acetic acid (7l): Dark brown solid, 50% yield. M.p. 201 °C; ^{1}H NMR (400 MHz, [D$_6$]DMSO): δ = 8.26 (d, J = 2.4 Hz, 1H), 8.20 (d, J = 8.8, 2.4 Hz, 1H), 8.03 (d, J = 8.8 Hz, 1H), 7.59 (d, J = 8.8 Hz, 2H), 7.03 (s, 1H), 6.51 (d, J = 8.8 Hz, 2H), 3.23 (m, 4H), 1.94 ppm (m, 4H); ^{13}C NMR (400 MHz, [D$_6$]DMSO): δ = 164.3, 147.8, 147.7, 134.4, 131.0, 127.0, 126.8, 125.8, 111.9, 47.7, 25.4 ppm; LC-MS (ESI+): m/z calcd for C$_{21}$H$_{18}$BrN$_5$O$_4$S: 515.03 [M+H]$^+$; found: 516.04, 518.02; AHPLC: t_R = 14.50 min, 93.49%.

2-(2-Bromo-5-nitrophenyl)-2-{2-[4-(4-morpholinophenyl)thiazol-2-yl]hydrazono}acetic acid (7m): Yellow solid, 73% yield. M.p. 191 °C; ^{1}H NMR (400 MHz, [D$_6$]DMSO): δ = 8.20 (d, J = 2.4 Hz, 1H), 8.19 (dd, J = 8.4, 2.8 Hz, 1H), 7.96 (d, J = 8.8 Hz, 1H), 7.59 (d, J = 9.2 Hz, 2H), 7.13 (s, 1H), 6.86 (d, J = 8.8 Hz, 2H), 3.65 (m, 4H), 3.06 ppm (m, 4H); ^{13}C NMR (100 MHz, [D$_6$]DMSO): δ = 164.5, 151.2, 147.9, 134.7, 131.2, 127.1, 115.4, 66.7, 48.6 ppm; LC-MS (ESI+): m/z calcd for C$_{21}$H$_{18}$BrN$_5$O$_5$S: 531.02 [M+H]$^+$; found: 532.04, 534.09; AHPLC: t_R = 12.60 min, 95.94%.

2-(2-Bromo-5-nitrophenyl)-2-(2-{4-[4-(dimethylamino)phenyl]thiazol-2-yl}hydrazono)acetic acid (7n): Yellow solid, 65% yield. M.p. 191 °C; ^{1}H NMR (400 MHz, [D$_6$]DMSO): δ = 8.26 (d, J = 2.8 Hz, 1H), 8.20 (dd, J = 8.8, 2.8 Hz, 1H), 8.03 (d, J = 8.8 Hz, 1H), 7.61 (d, J = 8.8 Hz, 2H), 7.08 (s, 1H), 6.70 (d, J = 8.8 Hz, 2H), 2.91 ppm (s, 6H); ^{13}C NMR (100 MHz, [D$_6$]DMSO): δ = 164.3, 150.4, 147.7, 134.4, 131.0, 126.9, 126.8, 125.8, 112.4, 40.4 ppm; LC-MS (ESI+): m/z calcd for C$_{19}$H$_{16}$BrN$_5$O$_4$S: 489.01 [M+H]$^+$; found: 490.19, 492.10; AHPLC: t_R = 10.44 min, 100%.

4-(2-{2-{[(2-Bromo-5-nitrophenyl)(carboxy)methylene]hydrazinyl}thiazol-4-yl)benzoic acid (7o): Yellow powder, 83% yield. M.p. 216 °C; ^{1}H NMR (400 MHz, [D$_6$]DMSO): δ = 8.30 (d, J = 2.4 Hz, 1H), 8.22 (dd, J = 9.2, 2.8 Hz, 1H), 8.05 (d, J = 8.8 Hz, 1H), 7.94 (m, 4H), 7.68 ppm (s, 1H); ^{13}C NMR (100 MHz, [D$_6$]DMSO): δ = 167.4, 164.1, 147.7, 138.4, 134.5, 130.9, 130.2, 130.1, 126.8, 126.0, 125.9, 109.0 ppm; LC-MS (ESI+): m/z calcd for C$_{18}$H$_{11}$BrN$_4$O$_6$S: 489.96; found: 491.04, 493.03 [M+H]$^+$, 445.03, 443.01 [M−NO$_2$]$^+$; AHPLC: t_R = 12.49 min, 95.47%.

2-(2-{2-{[(2-Bromo-5-nitrophenyl)(carboxy)methylene]hydrazinyl}thiazol-4-yl)benzoic acid (7p): Yellow solid, 68% yield. M.p. 183 °C; ^{1}H NMR (400 MHz, [D$_6$]DMSO): δ = 8.26 (d, J = 2.4 Hz, 1H), 8.19 (dd, J = 8.4, 2.8 Hz, 1H), 8.01 (d, J = 8.4 Hz, 1H), 7.65 (d, J = 7.6 Hz, 1H), 7.54 (m, 2H), 7.43 (m, 1H), 7.01 ppm (s, 1H); ^{13}C NMR (100 MHz, [D$_6$]DMSO): δ = 169.7, 164.3, 147.6, 134.4, 132.9, 131.1, 131.0, 130.3, 129.3, 128.6, 126.7, 125.9, 125.4 ppm; LC-MS (ESI+): m/z calcd for C$_{18}$H$_{11}$BrN$_4$O$_6$S: 489.96; found: 493.03, 491.04 [M+H]$^+$, 475.04, 473.06 [M−NO$_2$]$^+$; AHPLC: t_R = 12.43 min, 91.84%.

2-(2-Bromo-5-nitrophenyl)-2-{2-[4-(2-hydroxyphenyl)thiazol-2-yl]hydrazono}acetic acid (7q): Yellow solid, 78% yield. M.p. 198 °C; ^{1}H NMR (400 MHz, [D$_6$]DMSO): δ = 10.6 (s, 1H), 8.27 (d, J = 2.8 Hz, 1H), 8.17 (dd, J = 9.2, 2.8 Hz, 1H), 7.99 (d, J = 8.8 Hz, 1H), 7.73 (d, J = 7.2 Hz, 1H), 7.49 (s, 1H), 7.06 (t, J = 7.8 Hz, 1H), 6.81 (d, J = 8.0 Hz, 1H), 6.75 ppm (d, J = 7.4 Hz, 1H); ^{13}C NMR (100 MHz, [D$_6$]DMSO): δ = 164.1, 155.4, 147.7, 134.6, 130.9, 129.4, 127.9, 126.8, 126.2, 119.5, 117.1, 107.7 ppm; LC-MS (ESI+): m/z calcd for C$_{17}$H$_{11}$BrN$_4$O$_5$S: 461.96; found: 465.13, 463.08 [M+H]$^+$, 419.11, 417.13 [M−NO$_2$]$^+$; AHPLC: t_R = 15.38 min, 96.30%.

2-(2-Bromo-5-nitrophenyl)-2-{2-[4-(3-hydroxyphenyl)thiazol-2-yl]hydrazono}acetic acid (7r): Orange solid, 38% yield. M.p. 192 °C; ^{1}H NMR (400 MHz, [D$_6$]DMSO): δ = 9.37 (s, 1H), 8.22 (d, J = 2.8 Hz, 1H), 8.14 (dd, J = 8.8, 2.8 Hz, 1H), 7.96 (d, J = 8.8 Hz, 1H), 7.29 (s, 1H), 7.11 (m, 3H), 6.63 ppm (dd, J = 8.0, 1.6 Hz, 1H); ^{13}C NMR (100 MHz,

[D$_6$]DMSO): $\delta = 164.2$, 158.0, 147.7, 134.5, 131.0, 130.0, 126.8, 116.9, 115.4, 113.0 ppm; LC-MS (ESI+): m/z calcd for C$_{17}$H$_{11}$BrN$_4$O$_5$S: 461.96 [M+H]$^+$; found: 463.01, 464.99; AHPLC: $t_R = 12.86$ min, 89.97%.

2-(2-Bromo-5-nitrophenyl)-2-{2-[4-(4-hydroxyphenyl)thiazol-2-yl]hydra-zono}acetic acid (7s): Yellow solid, 51% yield. M.p. 158°C; ^{1}H NMR (400 MHz, [D$_6$]DMSO): $\delta = 9.60$ (s, 1H), 8.27 (d, $J = 2.4$ Hz, 1H), 8.22 (d, $J = 2.8$ Hz, 1H), 8.19 (d, $J = 2.4$ Hz, 1H), 8.03 (d, $J = 8.8$ Hz, 2H), 7.61 (d, $J = 8.8$ Hz, 2H), 7.16 (s, 1H), 6.76 ppm (d, $J = 8.4$, 2H); ^{13}C NMR (100 MHz, [D$_6$]DMSO): $\delta = 164.2$, 157.8, 147.7, 135.3, 134.5, 131.0, 127.4, 126.8, 126.2, 125.9, 115.8 ppm; LC-MS (ESI+): m/z calcd for C$_{17}$H$_{11}$BrN$_4$O$_5$S: 461.96; found: 462.95, 464.99 [M+H]$^+$, 416.93, 418.98 [M−NO$_2$]$^+$; AHPLC: $t_R = 12.44$ min, 91.32%.

2-(2-Bromo-5-nitrophenyl)-2-{2-[4-(3,4-dihydroxyphenyl)thiazol-2-yl]hy-drazono}acetic acid (7t): Yellow solid, 89% yield. M.p. 185°C; ^{1}H NMR (400 MHz, [D$_6$]DMSO): $\delta = 8.27$ (d, $J = 2.4$ Hz, 1H), 8.20 (s, 1H), 8.04 (s, 1H), 7.12 (m, 2H), 6.73 ppm (s, 1H); ^{13}C NMR (100 MHz, [D$_6$]DMSO): $\delta = 164.3$, 147.7, 146.0, 145.7, 134.5, 131.0, 126.8, 125.9, 117.5, 116.0, 113.8 ppm; LC-MS (ESI+): m/z calcd for C$_{17}$H$_{11}$BrN$_4$O$_6$S: 477.96; found: 479.14, 481.13 [M+H]$^+$, 433.13, 435.11 [M−NO$_2$]$^+$; AHPLC: $t_R = 11.31$ min, 100%.

2-(2-Bromo-5-nitrophenyl)-2-{2-[4-(3,4-dihydroxyphenyl)-5-methylthia-zol-2-yl]hydrazono}acetic acid (7u): Yellow solid, 78% yield. M.p. 177°C; ^{1}H NMR (400 MHz, [D$_6$]acetone): $\delta = 8.25$ (d, $J = 2.0$ Hz, 1H), 8.16 (dd, $J = 11.7$, 2.7 Hz, 1H), 7.96 (d, $J = 8.6$ Hz, 1H), 6.98 (s, 1H), 6.84 (dd, $J = 8.2$, 1.6 Hz 1H), 6.77 (d, $J = 8.2$ Hz, 1H), 2.33 ppm (s, 3H); ^{13}C NMR (100 MHz, [D$_6$]DMSO): $\delta = 165.1$, 146.6, 144.5, 144.0, 138.1, 135.4, 133.0, 129.1, 124.9, 123.9, 123.8, 119.1, 114.4, 114.0, 10.2 ppm; LC-MS (ESI+): m/z calcd for C$_{18}$H$_{13}$BrN$_4$O$_6$S: 491.97 [M+H]$^+$; found: 492.83, 494.81; AHPLC: $t_R = 11.45$ min, 95.10%.

General Procedure F—formation of the N-substituted nitroindazoles 1a–u from hydrazones 7: The appropriate hydrazone **7** (0.5 mmol), CuI (0.1 equiv), DMEDA (0.3 equiv), and Na$_2$CO$_3$ (2.2 equiv) were heated at reflux in a mixture of ethanol and water (1:1, 2 mL) for 2–12 h. The full conversion of the compound **7** into the desired product was monitored by HPLC-MS under the conditions described in the general section. The reaction mixture was allowed to cool to RT and neutralized with HCl (1 N), and the precipitate was filtered, dissolved in DMSO, and loaded onto a RP-Biotage column for further purification, as described in the general section above. For compounds **1a–h** see experimental data under General Procedure C.

1-[4-(2-Methoxyphenyl)thiazol-2-yl]-5-nitro-1H-indazole-3-carboxylic acid (1i): Yellow solid, 89% yield. M.p. 298°C; ^{1}H NMR (400 MHz, [D$_6$]DMSO): $\delta = 9.09$ (s, 1H), 8.81 (d, $J = 8.8$ Hz, 1H), 8.51 (d, $J = 9.6$ Hz, 1H), 8.24 (d, $J = 7.6$ Hz, 1H), 7.98 (s, 1H), 7.39 (t, $J = 7.8$ Hz, 1H), 7.18 (d, $J = 8.4$ Hz, 1H), 7.13 (t, $J = 7.4$ Hz, 1H), 3.98 ppm (s, 3H); ^{13}C NMR (100 MHz, [D$_6$]DMSO, recorded at 70°C): $\delta = 159.6$, 157.3, 148.4, 144.8, 140.9, 129.9, 129.7, 124.9, 124.3, 122.5, 121.2, 120.2, 115.3, 115.0, 112.5, 56.2 ppm; LC-MS (ESI+): m/z calcd for C$_{18}$H$_{12}$N$_4$O$_5$S: 396.05 [M+H]$^+$; found: 396.95; HRMS (ESI−): calcd for C$_{18}$H$_{11}$N$_4$O$_5$S: 395.0460 [M−H]$^-$; found: 395.0456; AHPLC: $t_R = 18.03$ min, 96.17%.

1-[4-(2,5-Dimethoxyphenyl)thiazol-2-yl]-5-nitro-1H-indazole-3-carbox-ylic acid (1j): White solid, 89% yield. M.p. 298°C; ^{1}H NMR (400 MHz, [D$_6$]DMSO): $\delta = 8.90$ (s, 1H), 8.73 (d, $J = 9.2$ Hz, 1H), 8.60 (d, $J = 9.2$ Hz, 1H), 7.99 (s, 1H), 7.61 (s, 1H), 7.07 (d, $J = 8.8$ Hz, 1H), 6.92 (d, $J = 8.8$ Hz, 1H), 3.88 (s, 3H), 3.79 ppm (s, 3H); LC-MS (ESI+): m/z calcd for C$_{19}$H$_{14}$N$_4$O$_6$S: 426.06 [M+H]$^+$; found: 426.91; HRMS (ESI+):

calcd for C$_{19}$H$_{15}$N$_4$O$_6$S: 427.07068; found: 427.07188 [M+H]$^+$, 449.05356 [M+Na]$^+$; AHPLC: $t_R = 17.84$ min, 99.43%.

1-[4-(2,4-Dichlorophenyl)thiazol-2-yl]-5-nitro-1H-indazole-3-carboxylic acid (1k): Light pink solid, 87% yield. M.p. 332°C; ^{1}H NMR (400 MHz, [D$_6$]DMSO): $\delta = 9.27$ (s, 1H), 8.65 (d, $J = 9.2$ Hz, 1H), 8.44 (d, $J = 9.6$ Hz, 1H), 8.09 (d, $J = 8.4$ Hz, 1H), 8.02 (s, 1H), 7.80 (d, $J = 2.0$ Hz, 1H), 7.61 ppm (dd, $J = 8.4$, 2.4 Hz, 1H); MS (ESI+): m/z calcd for C$_{17}$H$_8$Cl$_2$N$_4$O$_4$S: 433.96 [M+H]$^+$; found: 433.96, 435.98; HRMS (ESI−): calcd for C$_{17}$H$_7$Cl$_2$N$_4$O$_4$S: 432.9571; found: 434.970 [M−H]$^-$; AHPLC: $t_R = 20.89$ min, 97.49%.

5-Nitro-1-{4-[4-(pyrrolidin-1-yl)phenyl]thiazol-2-yl}-1H-indazole-3-car-boxylic acid (1l): Brown solid, 61% yield. M.p. 290°C; ^{1}H NMR (400 MHz, [D$_6$]DMSO): $\delta = 9.00$ (s, 1H), 8.87 (d, $J = 9.2$ Hz, 1H), 8.57 (dd, $J = 9.6$, 2.0 Hz, 1H), 7.83 (d, $J = 8.8$ Hz, 2H), 7.65 (s, 1H), 6.59 (d, $J = 8.8$ Hz, 2H), 3.31 (m, 4H), 2.02 ppm (m, 4H); ^{13}C NMR (100 MHz, [D$_6$]DMSO, recorded at 65°C): $\delta = 162.0$, 160.1, 153.5, 148.4, 145.2, 141.7, 140.9, 127.5, 124.6, 124.3, 121.3, 119.3, 115.6, 112.2, 107.2, 47.8, 25.3 ppm; LC-MS (ESI+): m/z calcd for C$_{21}$H$_{17}$N$_5$O$_4$S: 435.10 [M+H]$^+$; found: 436.10; HRMS (ESI+): calcd for C$_{21}$H$_{18}$N$_5$O$_4$S: 435.10740; found: 436.10594 [M+H]$^+$, 458.08842 [M+Na]$^+$; AHPLC: $t_R = 18.52$ min, 96.59%.

1-[4-(4-Morpholinophenyl)thiazol-2-yl]-5-nitro-1H-indazole-3-carboxyl-ic acid (1m): Brown solid, 62% yield. M.p. 270°C; ^{1}H NMR (400 MHz, [D$_6$]DMSO): $\delta = 8.90$ (s, 1H), 8.79 (d, $J = 9.6$ Hz, 1H), 8.51 (d, $J = 7.6$, 1.6 Hz, 1H), 7.89 (d, $J = 8.4$ Hz, 1H), 7.85 (s, 1H), 7.18 ppm (d, $J = 7.2$ Hz, 1H); LC-MS (ESI+): m/z calcd for C$_{21}$H$_{17}$N$_5$O$_5$S: 451.09 [M+H]$^+$; found: 451.97; HRMS (ESI+): calcd for C$_{21}$H$_{18}$N$_5$O$_5$S: 452.10232 [M+H]$^+$; found: 452.10334; AHPLC: $t_R = 15.21$ min, 95.95%.

1-{4-[4-(Dimethylamino)phenyl]thiazol-2-yl}-5-nitro-1H-indazole-3-car-boxylic acid (1n): Brown solid, 61% yield. M.p. 257°C; ^{1}H NMR (400 MHz, [D$_6$]DMSO): $\delta = 9.18$ (d, $J = 2.0$ Hz, 1H), 8.78 (d, $J = 8.8$ Hz, 1H), 8.47 (dd, $J = 9.2$, 2.4 Hz, 1H), 8.27 (s, 1H), 7.87 (d, $J = 9.2$ Hz, 2H), 7.61 (s, 1H), 6.80 (d, $J = 9.2$ Hz, 2H), 2.96 ppm (s, 6H); LC-MS (ESI+): m/z calcd for C$_{19}$H$_{15}$N$_5$O$_4$S: 409.08 [M+H]$^+$; found: 410.32; HRMS (ESI−): calcd for C$_{19}$H$_{16}$N$_5$O$_4$S: 410.09175 [M+H]$^+$; found: 410.09373; AHPLC: $t_R = 12.60$ min, 96.12%.

1-[4-(4-Carboxyphenyl)thiazol-2-yl]-5-nitro-1H-indazole-3-carboxylic acid (1o): Brown solid, 42% yield. M.p. 316°C; ^{1}H NMR (400 MHz, [D$_6$]DMSO): $\delta = 9.01$ (s, 1H), 8.93 (d, $J = 8.0$ Hz, 1H), 8.60 (d, $J = 8.8$ Hz, 1H), 8.27 (s, 1H), 8.22 (d, $J = 8.8$ Hz, 2H), 7.05 ppm (d, $J = 7.6$ Hz, 2H); ^{13}C NMR (100 MHz, [D$_6$]DMSO): $\delta = 167.4$, 160.9, 151.1, 145.0, 140.8, 137.5, 130.8, 130.3, 130.0, 129.1, 126.3, 124.8, 119.4, 115.7, 114.4, 110.0 ppm; LC-MS (ESI+): m/z calcd: 410.03 [M+H]$^+$; found: 411.04; HRMS (ESI+): calcd for C$_{18}$H$_{11}$N$_4$O$_6$S: 411.03938 [M+H]$^+$; found: 411.03859; AHPLC: $t_R = 13.71$ min, 95.83%.

1-[4-(2-Carboxyphenyl)thiazol-2-yl]-5-nitro-1H-indazole-3-carboxylic acid (1p): Yellow solid, 49% yield. M.p. 275°C; ^{1}H NMR (400 MHz, [D$_6$]DMSO): $\delta = 9.01$ (d, $J = 2.0$ Hz, 1H), 8.76 (d, $J = 9.6$ Hz, 1H), 8.52 (dd, $J = 9.6$, 2.4 Hz, 1H), 7.91 (s, 1H), 7.82 (d, $J = 7.6$ Hz, 1H), 7.70 (d, $J = 7.6$ Hz, 1H), 7.63 (dt, $J = 7.6$, 1.2 Hz, 1H), 7.54 ppm (t, $J = 7.6$ Hz, 1H); ^{13}C NMR (100 MHz, [D$_6$]DMSO): $\delta = 170.6$, 162.2, 159.7, 151.9, 148.2, 145.1, 140.9, 133.7, 132.6, 131.0, 129.7, 129.0, 128.9, 124.7, 124.2, 119.4, 115.4, 114.6 ppm; LC-MS (ESI+): m/z calcd for C$_{18}$H$_{10}$N$_4$O$_6$S: 410.03 [M+H]$^+$; found: 410.98; HRMS (ESI+): calcd for C$_{18}$H$_{11}$N$_4$O$_6$S: 411.03938; found: 411.03998 [M+H]$^+$, 433.02222 [M+Na]$^+$, 448.99526 [M+K]$^+$; AHPLC: $t_R = 13.83$ min, 96.71%.

1-[4-(2-Hydroxyphenyl)thiazol-2-yl]-5-nitro-1H-indazole-3-carboxylic acid (1q): Yellow solid, 96% yield. M.p. 299°C; ^{1}H NMR (400 MHz, [D$_6$]DMSO): $\delta = 10.55$ (s, 1H), 9.18 (s, 1H), 8.72 (d, $J = 8.8$ Hz, 1H),

8.45 (dd, $J=9.2$, 1.2 Hz, 1H), 8.16 (dd, $J=8.0$, 1.6 Hz, 1H), 7.98 (s, 1H), 7.16 (t, $J=15.5$ Hz, 1H), 4.00 (d, $J=8.4$ Hz, 1H), 6.92 ppm (t, $J=7.2$ Hz, 1H); ^{13}C NMR (100 MHz, [D$_6$]DMSO): $\delta=160.0$, 155.7, 150.1, 148.9, 144.1, 140.6, 129.5, 129.3, 123.9, 121.5, 120.6, 119.7, 116.8, 114.5, 114.1 ppm; LC-MS (ESI+): m/z calcd for C$_{17}$H$_{10}$N$_4$O$_5$S: 382.04 [M+H]$^+$; found: 382.78; HRMS (ESI−): calcd for C$_{17}$H$_{19}$N$_4$O$_5$S: 381.0299; found: 381.0286 [M−H]$^-$; AHPLC: $t_R=15.85$ min, 98.79%.

1-[4-(3-Hydroxyphenyl)thiazol-2-yl]-5-nitro-1H-indazole-3-carboxylic acid (1r): Yellow solid, 68% yield. M.p. >400°C; ^{1}H NMR (400 MHz, [D$_6$]DMSO): $\delta=9.23$ (s, 1H), 8.66 (d, $J=8.8$ Hz, 1H), 8.39 (d, $J=8.8$ Hz, 1H), 7.84 (s, 1H), 7.52 (s, 1H), 7.45 (d, $J=7.2$ Hz, 1H), 7.27 (t, $J=8.0$ Hz, 1H), 6.80 ppm (d, $J=7.2$ Hz, 1H); ^{13}C NMR (100 MHz, [D$_6$]DMSO): $\delta=161.2$, 159.9, 158.5, 158.4, 152.2, 143.9, 140.57, 135.3, 130.3, 124.6, 123.7, 121.8, 117.0, 115.9, 114.2, 113.4, 110.8 ppm; LC-MS (ESI+): m/z calcd for C$_{17}$H$_{10}$N$_4$O$_5$S: 382.04 [M+H]$^+$; found: 383.08; HRMS (ESI+): calcd for C$_{17}$H$_{11}$N$_4$O$_5$S: 383.04447; found: 383.04599 [M+H]$^+$, 405.02794 [M+Na]$^+$; AHPLC: $t_R=14.40$ min, 98.09%.

1-[4-(4-Hydroxyphenyl)thiazol-2-yl]-5-nitro-1H-indazole-3-carboxylic acid (1s): Brown solid, 87% yield. M.p. 231°C; ^{1}H NMR (400 MHz, [D$_6$]DMSO): $\delta=9.73$ (s, 1H), 8.99 (d, $J=2.0$ Hz, 1H), 8.91 (d, $J=9.2$ Hz, 1H), 8.56 (dd, $J=9.6$, 2.0 Hz, 1H), 7.90 (d, $J=8.8$ Hz, 2H), 7.79 (s, 1H), 6.88 ppm (d, $J=8.4$ Hz, 2H); ^{13}C NMR (100 MHz, [D$_6$]DMSO): $\delta=160.4$, 158.4, 152.7, 148.7, 148.1, 145.1, 140.9, 127.9, 125.1, 124.8, 124.3, 119.5, 116.1, 115.7, 109.1 ppm; MS (ESI+): m/z calcd for C$_{17}$H$_{10}$N$_4$O$_5$S: 382.04 [M+H]$^+$; found: 382.97; HRMS (ESI+): calcd for C$_{17}$H$_{11}$N$_4$O$_5$S: 383.04447; found: 383.04629 [M+H]$^+$, 405.02794 [M+Na]$^+$; AHPLC: $t_R=14.09$ min, 95.07%.

1-[4-(3,4-Dihydroxyphenyl)thiazol-2-yl]-5-nitro-1H-indazole-3-carboxylic acid (1t): Brown solid, 72% yield. M.p. 258°C; ^{1}H NMR (400 MHz, [D$_6$]DMSO): $\delta=9.27$ (br s, 1H), 9.09 (br s, 1H), 9.00 (s, 1H), 8.87 (d, $J=9.6$ Hz, 1H), 8.56 (d, $J=9.2$ Hz, 1H), 7.72 (s, 1H), 7.45 (s, 1H), 7.37 (d, $J=8.4$ Hz, 1H), 6.85 ppm (d, $J=8.4$ Hz, 1H); ^{13}C NMR (100 MHz, [D$_6$]DMSO): $\delta=160.2$, 152.8, 146.6, 145.9, 145.0, 125.5, 124.7, 119.5, 118.0, 116.3, 115.4, 113.9, 109.1 ppm; LC-MS (ESI+): m/z calcd for C$_{17}$H$_{10}$N$_4$O$_6$S: 398.03; found: 399.14 [M+H]$^+$, 381.16 [M−OH]$^+$; HRMS (ESI+): calcd for C$_{17}$H$_{11}$N$_4$O$_6$S: 399.0394 [M+H]$^+$; found: 399.0404; AHPLC: $t_R=12.71$ min, 100%.

1-[4-(3,4-Dihydroxyphenyl)-5-methylthiazol-2-yl]-5-nitro-1H-indazole-3-carboxylic acid (1u): Yellow solid, 67% yield. M.p. 244°C; ^{1}H NMR (400 MHz, [D$_6$]DMSO): $\delta=9.09$ (s, 1H), 8.70 (d, $J=9.2$ Hz, 1H), 8.37 (dd, $J=9.6$, 2.4 Hz, 1H), 7.17 (d, $J=1.6$ Hz, 1H), 7.01 (dd, $J=1.6$ Hz, 1H), 7.79 (d, $J=8.4$ Hz, 1H), 2.49 ppm (s, 3H); ^{13}C NMR (100 MHz, [D$_6$]DMSO): $\delta=156.4$, 148.1, 145.9, 145.8, 144.0, 140.3, 125.9, 123.7, 122.7, 120.8, 119.8, 116.3, 115.9, 114.4, 12.7 ppm; LC-MS (ESI+): m/z calcd for C$_{18}$H$_{12}$N$_4$O$_6$S: 412.05 [M+H]$^+$; found: 413.09; HRMS (ESI+): calcd for C$_{18}$H$_{13}$N$_4$O$_6$S: 413.05503 [M+H]$^+$; found: 413.05543; AHPLC: $t_R=13.23$ min, 97.63%.

Biology

Cell growth assay: CRL-2813 human melanoma cells were grown as per ATCC instructions (http://www.atcc.org). Cells were plated in standard 96-well tissue culture plates and treated with test compounds (dissolved in DMSO) at final concentrations of 17.14, 5.14, 1.54 and 0.46 μM. On the fifth day after addition of the compound, the plates were fixed with cold trichloroacetic acid (10%) at 4°C for 1 h, washed five times with water, and air-dried overnight at 4°C. Sulforhodamine B (SRB) in acetic acid (1%) was added to each well, and incubation at RT was carried out for 30 min. Unbound dye was removed by washing the wells extensively with water containing acetic acid (1%), and the plates were air-dried overnight at

4°C. TRIS-base (10 mm) was added to each well, and the plates were read at 520 nm with a Thermo Scientific MultiScan FC plate reader.[45a]

Western blotting (WB): The WB analysis was performed as described.[45a] Briefly, CRL-2813 cells were seeded in 15 cm plates and treated with DMSO or the tested compounds at final concentrations of 50 or 25 μM for 8 h at >75% confluency. Cells were washed once with ice-cold PBS and were lysed. Equal protein samples were separated by SDS-PAGE, and WB analysis was performed as described. The following antibodies were utilized: cyclin D1 (Santa Cruz Biotechnology, sc-8396), survivin (Cell Signaling, #2808), mTOR (Cell Signaling, #2983), p70S6K (Santa Cruz Biotechnology, sc-8418), eIF4E (Cell Signaling, #9742), P-eIF4E (Cell Signaling, #9741), T-4E-BP1 (Cell Signaling, #9452), P-4E-BP1 (Cell Signaling, #9459), β-actin (Santa Cruz Biotechnology, sc-1615).

RT-PCR: RT-PCR analysis was carried out essentially as described by Chen (2011).[45a] Briefly, CRL-2813 cells were incubated for 6 h in the presence of the tested compounds in a 96-well plate at final concentrations of 25 and 50 μM. Total RNA was extracted with a Fast-Lane Cell One-Step RT-PCR Kit (Qiagen, Valencia, CA) according to the manufacturer's protocol. Contaminating DNA was removed by DNase I treatment. One-step real-time PCR was performed with a Bio-Rad iCycler IQ5 system and use of a B-R 1-Step SYBR Green qRT-PCR Kit (Quanta BioSciences, Gaithersburg, MD) according to the manufacturer's specifications. The thermal cycler conditions were as follows: 10 min at 50°C, hold for 5 min at 95°C, followed by two-step PCR for 45 cycles of 95°C for 15 s followed by 60°C for 30 s. All PCR reactions were performed in triplicate in at least two independent PCR runs. Mean values of these repeated measurements were used for calculation. To calibrate the results, all the transcript quantities were normalized to 18S rRNA. The following primers were used in real-time PCR reactions: for cyclin D1: Hs_CCND1_1_SG QuantiTect Primer Assay, QT00495285, for survivin: Hs_BIRC5_2_SG QuantiTect Primer Assay, QT01679664, for p70S6K: Hs_RPS6KB2_1_SG QuantiTect Primer Assay, QT00086632, and Human 18S rRNA (5′-CGGCGA CGACCC ATTCGA AC-3′ and 5′-GAATCG AACCCT GATTCC CCGTC-3′).

[1] a) L. Lo Conte, C. Chothia, J. Janin, *J. Mol. Biol.* **1999**, *285*, 2177–2198; b) J. C. Fuller, N. J. Burgoyne, R. M. Jackson, *Drug Discovery Today* **2009**, *14*, 155–161.

[2] a) D. E. Scott, M. T. Ehebauer, T. Pukala, M. Marsh, T. L. Blundell, A. R. Venkitaraman, C. Abell, M. Hyvönen, *ChemBioChem* **2013**, *14*, 332–342; b) S. Surade, T. L. Blundell, *Chem. Biol.* **2012**, *19*, 42–50; c) D. Gonzalez-Ruiz, H. Gohlke, *Curr. Med. Chem.* **2006**, *13*, 2607–2625; d) V. Azzarito, K. Long, N. S. Murphy, A. J. Wilson, *Nat. Chem.* **2013**, *5*, 161–173; e) A. D. Thompson, A. Dugan, J. E. Gestwicki, A. K. Mapp, *ACS Chem. Biol.* **2012**, *7*, 1311–1320.

[3] a) A. J. Wilson, *Chem. Soc. Rev.* **2009**, *38*, 3289–3300; b) G. Zinzalla, D. E. Thurston, *Future Med. Chem.* **2009**, *1*, 65–93.

[4] a) P. Buchwald, *IUBMB Life* **2010**, *62*, 724–731; b) A. Whitty, G. Kumaravel, *Nat. Chem. Biol.* **2006**, *2*, 112–118; c) T. Berg, *Angew. Chem.* **2003**, *115*, 2566–2586; *Angew. Chem. Int. Ed.* **2003**, *42*, 2462–2481.

[5] N. Sonenberg, A. G. Hinnebusch, *Cell* **2009**, *136*, 731–745.

[6] A. C. Gingras, B. Raught, N. Sonenberg, *Annu. Rev. Biochem.* **1999**, *68*, 913–963.

[7] R. J. Jackson, C. U. Hellen, T. V. Pestova, *Nat. Rev. Mol. Cell Biol.* **2010**, *11*, 113–127.

[8] L. S. Hiremath, N. R. Webb, R. E. Rhoads, *J. Biol. Chem.* **1985**, *260*, 7843–7849.

[9] J. D. Richter, N. Sonenberg, *Nature* **2005**, *433*, 477–480.

[10] N. Sonenberg, *Curr. Opin. Cell Biol.* **1993**, *5*, 955–960.

[11] C. A. Hoeffer, K. K. Cowansage, E. C. Arnold, J. L. Banko, N. J. Moerke, R. Rodriguez, E. K. Schmidt, E. Klosi, M. Chorev, R. E. Lloyd, P. Pierre, G. Wagner, J. E. LeDoux, E. Klann, *Proc. Natl. Acad. Sci. USA* **2011**, *108*, 3383–3388.

[12] a) B. J. O'Roak, L. Vives, W. Fu, J. D. Egertson, I. B. Stanaway, I. G. Phelps, G. Carvill, A. Kumar, C. Lee, K. Ankenman, J. Munson, J. B. Hiatt, E. H. Turner, R. Levy, D. R. O'Day, N. Krumm, B. P. Coe, B. K. Martin, E. Borenstein, D. A. Nickerson, H. C. Mefford, D. Doherty, J. M. Akey, R. Bernier, E. E. Eichler, J. Shendure, *Science* **2012**, *338*, 1619–1622; b) C. G. Gkogkas, A. Khoutorsky, I. Ran, E. Rampakakis, T. Nevarko, D. B. Weatherill, C. Vasuta, S. Yee, M. Truitt, P. Dallaire, F. Major, P. Lasko, D. Ruggero, K. Nader, J. C. Lacaille, N. Sonenberg, *Nature* **2013**, *493*, 371–377.

[13] a) S. A. Connor, C. A. Hoeffer, E. Klann, P. V. Nguyen, *Learn. Mem.* **2011**, *18*, 207–220; b) I. Napoli, V. Mercaldo, P. P. Boyl, B. Eleuteri, F. Zalfa, S. De Rubeis, D. Di Marino, E. Mohr, M. Massimi, M. Falconi, W. Witke, M. Costa-Mattioli, N. Sonenberg, T. Achsel, C. Bagni, *Cell* **2008**, *134*, 1042–1054.

[14] a) Q. Yang, K. Inoki, E. Kim, K. L. Guan, *Proc. Natl. Acad. Sci. USA* **2006**, *103*, 6811–6816; b) P. T. Tsai, C. Hull, Y. Chu, E. Greene-Colozzi, A. R. Sadowski, J. M. Leech, J. Steinberg, J. N. Crawley, W. G. Regehr, M. Sahin, *Nature* **2012**, *488*, 647–651; c) T. Kobayashi, O. Minowa, Y. Sugitani, S. Takai, H. Mitani, E. Kobayashi, T. Noda, O. Hino, *Proc. Natl. Acad. Sci. USA* **2001**, *98*, 8762–8767.

[15] R. J. Kelleher III, M. F. Bear, *Cell* **2008**, *135*, 401–406.

[16] a) A. Amiri, W. Cho, J. Zhou, S. G. Birnbaum, C. M. Sinton, R. M. McKay, L. F. Parada, *J. Neurosci.* **2012**, *32*, 5880–5890; b) J. Zhou, L. F. Parada, *Curr. Opin. Neurobiol.* **2012**, *22*, 873–879; c) C. H. Kwon, B. W. Luikart, C. M. Powell, J. Zhou, S. A. Matheny, W. Zhang, Y. Li, S. J. Baker, L. F. Parada, *Neuron* **2006**, *50*, 377–388; d) B. D. Auerbach, E. K. Osterweil, M. F. Bear, *Nature* **2011**, *480*, 63–68.

[17] D. Ehninger, S. Han, C. Shilyansky, Y. Zhou, W. Li, D. J. Kwiatkowski, V. Ramesh, A. J. Silva, *Nat. Med.* **2008**, *14*, 843–848.

[18] A. Sharma, C. A. Hoeffer, Y. Takayasu, T. Miyawaki, S. M. McBride, E. Klann, R. S. Zukin, *J. Neurosci.* **2010**, *30*, 694–702.

[19] a) A. R. Tee, D. C. Fingar, B. D. Manning, D. J. Kwiatkowski, L. C. Cantley, J. Blenis, *Proc. Natl. Acad. Sci. USA* **2002**, *99*, 13571–13576; b) Y. J. Kang, M. K. Lu, K. L. Guan, *Cell Death Differ.* **2011**, *18*, 133–144.

[20] a) N. J. Moerke, H. Aktas, H. Chen, S. Cantel, M. Y. Reibarkh, A. Fahmy, J. D. Gross, A. Degterev, J. Yuan, M. Chorev, J. A. Halperin, G. Wagner, *Cell* **2007**, *128*, 257–267; b) L. Chen, B. H. Aktas, Y. Wang, X. He, R. Sahoo, N. Zhang, S. Denoyelle, E. Kabha, H. Yang, R. Y. Freedman, J. G. Supko, M. Chorev, G. Wagner, J. A. Halperin, *Oncotarget* **2012**, *3*, 869–881.

[21] a) M. N. Chaur, D. Collado, J. M. Lehn, *Chem. Eur. J.* **2011**, *17*, 248–258; b) A. Brandt, M. Cerquetti, G. B. Corsi, G. Pascucci, A. Simeoni, P. Martelli, U. Valcavi, *J. Med. Chem.* **1987**, *30*, 764–767.

[22] H. Cerecetto, A. Gerpe, M. Gonzalez, V. J. Aran, C. O. de Ocariz, *Mini-Rev. Med. Chem.* **2005**, *5*, 869–878.

[23] H. W. Gschwend (Ciba Geigy Co.), US 3681382 A, **1972**.

[24] G. Corsi, G. Palazzo, *J. Med. Chem.* **1976**, *19*, 778–783.

[25] Y. K. Lee, D. J. Parks, T. Lu, T. V. Thieu, T. Markotan, W. Pan, D. F. McComsey, K. L. Milkiewicz, C. S. Crysler, N. Ninan, M. C. Abad, E. C. Giardino, B. E. Maryanoff, B. P. Damiano, M. R. Player, *J. Med. Chem.* **2008**, *51*, 282–297.

[26] R. Gomez, S. J. Jolly, T. Williams, J. P. Vacca, M. Torrent, G. McGaughey, M. T. Lai, P. Felock, V. Munshi, D. Distefano, J. Flynn, M. Miller, Y. Yan, J. Reid, R. Sanchez, Y. Liang, B. Paton, B. L. Wan, N. Anthony, *J. Med. Chem.* **2011**, *54*, 7920–7933.

[27] X. Zhang, F. Song, G. H. Kuo, A. Xiang, A. C. Gibbs, M. C. Abad, W. Sun, L. C. Kuo, Z. Sui, *Bioorg. Med. Chem. Lett.* **2011**, *21*, 4762–4767.

[28] a) B. S. Brown, R. Keddy, R. J. Perner, S. DiDomenico, J. R. Koenig, T. K. Jinkerson, S. M. Hannick, H. A. McDonald, B. R. Bianchi, P. Honore, P. S. Puttfarcken, R. B. Moreland, K. C. Marsh, C. R. Faltynek, C. H. Lee, *Bioorg. Med. Chem. Lett.* **2010**, *20*, 3291–3294; b) V. Bodmer-Narkevitch, N. J. Anthony, V. Cofre, S. M. Jolly, K. L. Murphy, R. W. Ransom, D. R. Reiss, C. Tang, T. Prueksaritanont, D. J. Pettibone, M. G. Bock, S. D. Kuduk, *Bioorg. Med. Chem. Lett.* **2010**, *20*, 7011–7014.

[29] T. Okuzumi, G. S. Ducker, C. Zhang, B. Aizenstein, R. Hoffman, K. M. Shokat, *Mol. BioSyst.* **2010**, *6*, 1389–1402.

[30] A. E. Kümmerle, M. Schmitt, S. V. Cardozo, C. Lugnier, P. Villa, A. B. Lopes, N. C. Romeiro, H. Justiniano, M. A. Martins, C. A. Fraga, J. J. Bourguignon, E. J. Barreiro, *J. Med. Chem.* **2012**, *55*, 7525–7545.

[31] F. Delbecq, G. Cordonnier, N. Pommery, D. Barbry, J. P. Henichart, *Bioorg. Med. Chem. Lett.* **2004**, *14*, 1119–1121.

[32] A. Merijanian, G. M. Sharma, J. Moushati, K. Gunderson, *J. Org. Chem.* **1986**, *51*, 543–545.

[33] A. Schmidt, A. Beutler, T. Habeck, T. Mordhorst, B. Snovydovych, *Synthesis* **2006**, 1882–1894.

[34] a) K. Lukin, M. C. Hsu, D. Fernando, M. R. Leanna, *J. Org. Chem.* **2006**, *71*, 8166–8172; b) A. Schmidt, A. Beutler, B. Snovydovych, *Eur. J. Org. Chem.* **2008**, 4073–4095.

[35] J. Kempson in *Name Reactions in Heterocyclic Chemistry II* (Ed: J. J. Li), Wiley, Hoboken, **2011**, pp. 299–309.

[36] J. Schröder, A. Henke, H. Wenzel, H. Brandstetter, H. G. Stammler, A. Stammler, W. D. Pfeiffer, H. Tschesche, *J. Med. Chem.* **2001**, *44*, 3231–3243.

[37] a) A. A. Avetissyan, L. A. Khchatryan, R. F. Papoyan, *Hayastani Kim. Handes* **2010**, *63*, 121; b) A. P. Novikova, N. M. Perova, L. G. Egorova, E. I. Bragina, *Khim. Geterotsikl. Soedin.* **1991**, *6*, 843–846.

[38] a) M. Kidwai, R. Venkataramanan, B. Dave, *J. Heterocycl. Chem.* **2002**, *39*, 1045–1047; b) P. Gothwal, Y. K. Srivastava, *Chem. Sin.* **2012**, *3*, 318–322.

[39] P. Magiatis, P. Polychronopoulos, A. L. Skaltsounis, O. Lozach, L. Meijer, D. B. Miller, J. P. O'Callaghan, *Neurotoxicol. Teratol.* **2010**, *32*, 212–219.

[40] J. Hlaváč, M. Soural, P. Hradil, I. Fryšová, J. Slouka, *J. Heterocycl. Chem.* **2004**, *41*, 633–636.

[41] a) J. C. Antilla, J. M. Baskin, T. E. Barder, S. L. Buchwald, *J. Org. Chem.* **2004**, *69*, 5578–5587; b) J. C. Antilla, A. Klapars, S. L. Buchwald, *J. Am. Chem. Soc.* **2002**, *124*, 11684–11688; c) T. Kylmälä, S. Udd, J. Tois, R. Franzén, *Tetrahedron Lett.* **2010**, *51*, 3613–3615.

[42] M. Ishikawa, Y. Hashimoto, *J. Med. Chem.* **2011**, *54*, 1539–1554.

[43] K. H. T. Paraiso, Y. Xiang, V. W. Rebecca, E. V. Abel, Y. A. Chen, A. C. Munko, E. Wood, I. V. Fedorenko, V. K. Sondak, A. R. A. Anderson, A. Ribas, M. Dalla Palma, K. L. Nathanson, J. M. Koomen, J. L. Messina, K. S. M. Smalley, *Cancer Res.* **2011**, *71*, 2750–2760.

[44] H. Aktas, H. Cai, G. M. Cooper, *Mol. Cell. Biol.* **1997**, *17*, 3850–3857.

[45] a) T. Chen, D. Ozel, Y. Qiao, F. Harbinski, L. Chen, S. Denoyelle, X. He, N. Zvereva, J. G. Supko, M. Chorev, J. A. Halperin, B. H. Aktas, *Nat. Chem. Biol.* **2011**, *7*, 610–616; b) H. Bai, T. Chen, J. Ming, H. Sun, P. Cao, D. N. Fusco, R. T. Chung, M. Chorev, Q. Jin, B. H. Aktas, *ChemBioChem* **2013**, *14*, 1255–1262.

[46] Z. Diwu, C. Beachdel, D. H. Klaubert, *Tetrahedron Lett.* **1998**, *39*, 4987–4990.

[47] C. Herbivo, A. Comel, G. Kirsch, M. M. M. Raposo, *Tetrahedron* **2009**, *65*, 2079–2086.

[48] R. L. N. Harris, J. L. Huppatz, *Aust. J. Chem.* **1977**, *30*, 2225–2240.

[49] L. C. King, G. K. Ostrum, *J. Org. Chem.* **1964**, *29*, 3459–3461.

[50] K. Koch, M. S. Biggers, *J. Org. Chem.* **1994**, *59*, 1216–1218.

[51] J. Pospíšil, C. Müller, A. Fürstner, *Chem. Eur. J.* **2009**, *15*, 5956–5968.